University of Essex

Research Repository

Towards the Development of an Efficient Nonlinear Controller for ART against HIV Infection

Accepted for publication in the Journal of Mathematical Biology

Research Repository link: https://repository.essex.ac.uk/43879/

Please note:

Changes made as a result of publishing processes such as copy-editing, formatting and page numbers may not be reflected in this version. For the definitive version of this publication, please refer to the published source. You are advised to consult the published version if you wish to cite this paper.
https://doi.org/10.1007/s00285-026-02471-6

www.essex.ac.uk

University of Essex

Towards the Development of Efficient Nonlinear Controller for ART and cART against HIV Infection

Muhammad Arsalan[a,b], Sadiq Muhammad Tariq[c], Abubakar Rafique[a], Ahmad Almogren[d], and Xiaojun Yu[a,*]

[a] *School of Automation, Northwestern Polytechnical University, Xi'an, 710072, China*

[b] *Department of Electrical Engineering, University of Engineering and Technology, Lahore, 54890, Pakistan*

[c] *School of Computer Science and Electronic Engineering, University of Essex, Wivenhoe Park, Colchester CO4 3SQ, United Kingdom; ORCID: 0000-0002-7410-5951*

[d] *Department of Computer Science, College of Computer and Information Sciences, King Saud University, Riyadh 11633, Saudi Arabia*

Abstract

The Human Immuno-deficiency Virus (HIV) is responsible for attacking the CD4+ T cells present in human blood and causes the human immune system to become vulnerable for numerous contagious and opportunistic diseases. It is hence pertinent to curb the spread of HIV infection using anti-HIV drugs. This study integrates sigmoid function with conventional sliding mode control and incorporate it within the framework of multi-objective optimal model predictive controller to reduce the impact of HIV infection through anti-retro-viral therapy. The proposed algorithm is designed using a deterministic HIV-human immune system model that also includes the dynamics of cytotoxic T-lymphocytes precursor and effector cells. The research work provides the detailed design of nonlinear sigmoid based SMC controller and its Lyapunov theory based stability analysis. This designed controller is then integrated within the framework of MPC. Simulation level dosage bounds derived from the considered reference values for anti-HIV drug dosage has been realized to explicate and understand the relationship between administered dosage and control inputs. To validate the superior performance of the proposed controller, the results are compared to that of recently proposed nonlinear backstepping, state-feedback and synergetic controllers. Lastly, the proposed control algorithm is also evaluated using a three-state, three-input HIV model to examine

*Corresponding Author

Email address: m_arsalan@mail.nwpu.edu.cn, XJYU@nwpu.edu.cn, tariq.sadiq@mail.nwpu.edu.cn, and abubakar157@mail.nwpu.edu.cn (Muhammad Arsalan[a,b], Sadiq Muhammad Tariq[c], Abubakar Rafique[a], Ahmad Almogren[d], and Xiaojun Yu[a,*])

September 12, 2026

its applicability to combination anti-retro-viral therapy (cART). The simulations demonstrate that the proposed sigmoid SMC-MPC framework can regulate the modeled drug inputs while simultaneously improving the simulated CD4+ T-cell response and suppressing viral load. The results are intended to demonstrate the algorithmic performance of the proposed nonlinear control framework within the considered mathematical models. Importantly, this study is simulation-based and does not constitute a clinical treatment strategy or a recommendation for automated administration of anti-retro-viral drugs. The simulations are performed using MATLAB/Simulink. The observations and results presented in this study are also analyzed to substantiate the need of nonlinear feedback controllers to limit the amount of administered treatment burden to effectively and efficiently curb HIV advancement. Results showed that the proposed hybrid sigmoid SMC-MPC approach effectively lowered the initial drug dosage requirements by 30%. Whereas, the reduction in final steady state dosage has been reduced by upto 70% while reducing the convergence time of viral load by 14%. Similarly, the convergence time of healthy CD4 +T cell count, to the desired reference level, has been reduced by 26.8%. These results indicate favorable algorithmic performance within the considered simulation framework.

Keywords: Human Immunodeficiency Virus (HIV), Acquired Immune Deficiency Syndrome (AIDS), $CD4^{+}T$ Receptor Cells, Backstepping, State-feedback, Synergetic, Anti-Retro-Viral Therapy (ART), Combination Anti-Retro-Viral Therapy (cART)

---

1. Introduction

Human Immunodeficiency Virus (HIV) is a type of virus that attacks and compromises the immunity of the infected person. Lymphocytes, made up of B-cells and CD4 +T cells (or simply T-cells), are an important constituent of white blood cells. These cells produce anti-bodies against viruses, bacteria and other foreign invaders, and they also destroy the infected cells in human body that may aid in the spread of infection [1]. The HIV directly attacks the Lymphocytes (preferentially T-cells) and binds itself to their surface and starts replicating its copies, resulting in the destruction of T-cells in the process. The newly generated copies then attack other T-cells and if left unchecked, the population of CD4 +T cells exponentially decreases, resulting in a weaken immune system and a feeble human body [2, 3].

Based on symptoms, the HIV infection can be classified into three stages (Figure 1: Stages of HIV Infection). Acute HIV infection; is the earliest stage of HIV in which the infected person may

exhibit flu-like symptoms. Other signs include headache, fatigue, sore throat, fever, rashes, ulcers and swollen lymph nodes. The flu-like symptoms stop manifestation after two to four weeks and the disease advances to asymptotic stage [4, 5]. This stage is also called clinical latency stage, as the person affected by the virus may not show any HIV related symptoms at all. Although HIV infection is incurable, but if Anti-Retro-Viral Therapy (ART) is initiated during the first two stages of the infection, it is still manageable, and the infected may lead a long and healthy life [4]. It may take around ten or more years by the disease to advance to the next stage [6, 7].

For the early diagnosis of HIV, any of the Antibody tests, Antigen tests or Nucleic Acid Test (NAT) may be employed [8]. CD4 count test (or T-cell count) is not generally employed for initial detection of HIV. However, once HIV is diagnosed, then CD4 count is utilized globally to analyze the advancement of HIV [9]. For Stage-1 HIV, the CD4 count generally remains greater than 500 $cells\ mm^{-3}$. Whereas, for Stage-2 HIV, the range of CD4 count remains between 200 500 $cells\ mm^{-3}$. If the CD4 count drops below 200 $cells\ mm^{-3}$, then it is considered as the indication that the HIV infection has advanced to Stage-3, which is also termed as: Acquired Immune Deficiency Syndrome (AIDS) [8, 10, 11]. Numerous infection and contagious diseases may now attack the infected person as the immune system becomes exceptionally weak [12, 13]. The symptoms may include fever, diarrhea, muscular pain, ulcers, sores, blotches, swollen lymph nodes, tuberculosis, pneumonia, etc. [6, 14].

It is hence pertinent to control and manage the disease during its first two stages. Protease inhibitors (PI) are a class of drugs administered against HIV to contain the disease in its early stages by inhibiting the production of a protein, protease, in them [15]. The newly produced virus copies require protease to fully mature and become infectious. Similarly, fusion inhibitors (FI) are another class of drugs that prevent the HIV particles to fuse on the surface of CD4+ T cells for infection initiation. Whereas, the HIV particles replicate themselves through an infected host cell using a process called reverse transcriptase. Hence, reverse transcriptase inhibitors (RTI) are another class of potent anti-HIV drugs that directly interrupt the replication cycle of the virus particles. Thus, by impeding their development, these drugs result in the indirect reduction of viral load as the non-infectious viruses die at a natural rate [15]. Though efficient and effective in anti-retro-viral therapy, these drugs have adverse side effects. For example, the drug Indinavir may cause kidney stones, hyperglycemia, diabetes, heart attacks, hemolytic anemia, etc. [16]. Similarly, Atazanavir is another protease inhibitor, that may cause symptoms like hyperbilirubinemia, jaundice, scleral icterus,

cholelithiasis, nephrolithiasis, etc. [16]. Therefore, an automated drug injection and regulation mechanism is crucial for anti-retro-viral therapy to avoid drug over dosage and to limit their side effects.

Substantial research has been carried out to understand the effect of HIV infection on $CD4+T$ cells. As a result, numerous mathematical models have been developed to explain this complex relation between the HIV particles and the T cells. These models not only enable the researchers to study the long-lasting effect of HIV on the human immune system, but they also enable them to study the response of numerous classes of drugs on HIV as well as the immune system. The most basic and minimal mathematical model is based on three basic variables, that are healthy T cells, infected T cells and the free virus particles in blood stream [17, 18]. A similar approach based on the same three variables was utilized in [19, 20] and [21], however, protease inhibitor was considered as the main anti-HIV drug in the former one and reverse transcriptase inhibitor (another class of ART drug) was utilized to manage HIV in the later one. All these minimal models are based on the work of Wodarz and Nowak [22].

The CD8+T lymphocytes, mostly referred as Cytotoxic T-Lymphocytes Effectors (CTLEs), are the cells tasked to destroy the infection-spreading cells from the human body. The minimal model does not include the effect of CTLEs on HIV dynamics[23]. This effect was included in the study by [23] and [24]. The CTLEs are however, not activated immediately to kill the infected T cells. The dynamics of CTLEs along with their activation was considered in [25, 26]. Similarly, the process of HIV reproduction involves certain steps, before the virus becomes fully mature to infect the lymphocytes [27, 28]. The inclusion of virus activation process and CTLE activation process in the Immune System HIV dynamics are hence pivotal in the determination of anti-HIV drug dosage.

Although, for an HIV infected person, the viral load can never reduce to zero, yet the ultimate goal of ART is to minimize the viral load as much as possible [25]. Hence, using the nonlinear model for HIV-immune system dynamics, researchers have recently developed control algorithms to reduce this viral load [29, 30]. Due to the adverse side affects of the protease inhibitors, researchers have opted optimal based controllers to limit the drug over-dosage [28]. Yet, most of these optimal controllers have to linearize the highly nonlinear HIV-immune system model for the successful execution and design of these controllers [24, 18]. Linearization of the nonlinear system ensures the optimal performance of the control system near a selected certain equilibrium point of the system, but the global stability of the overall system is generally compromised [17, 27, 31]. Moreover, the

convergence of the system to some other, undesired equilibrium point also becomes a possibility, jeopardizing the performance and benevolence of the control system [30, 32].

The information lost during the linearization of a nonlinear system gravely affects the performance of linear controllers. However, such issues dont crop up if nonlinear controllers are used instead [33]. Recently, [19] has suggested Lyapunov stability theory based nonlinear synergetic and state-feedback controllers for the application of ART using minimal model. Similarly, sliding mode controller has been utilized for the minimal model as well to efficiently reduce viral load [21]. However, these controllers havent been utilized for higher order, more realistic nonlinear HIV dynamical system. Similarly, even though numerous studies have proposed optimization based approaches for ART, yet none of them considered the minimization of the administered drug dosage to limit the harmful toxic side effects of the treatment therapy.

This study aims to improve the nonlinear HIV immune system dynamical model by incorporating the effect of protease inhibitor drug dosage. The viral load is then reduced using ART and feedback-based, multi-objective, nonlinear sigmoid SMC-based MPC algorithm. The proposed multi-objective approach is designed to maximize healthy CD4+ T cell count and minimize viral load and control input drug dosage to indirectly minimize treatment induced toxicity. Moreover, the study also develops a relationship between the conventional drug dosage and the control input. To validate the effectiveness, superiority and stability of the designed control algorithm, its performance is compared to that of conventional linear and nonlinear controllers including recently proposed synergetic, statefeedback and backstepping control algorithms [19, 34]. Though more toxic and harmful than ART, cART is however more effective against infectious advancements of HIV. To further prove the adaptability and versatility of the proposed smooth SMC-based MPC algorithm, it is also employed for cART against HIV using three-state and three-input minimal system model. The following contributions are proposed in this research work:

1. Improvement of existing nonlinear HIV immune system dynamical model
2. Proposition of novel sigmoid-SMC based MPC optimizer to control the nonlinear HIV immune system dynamical model by incorporating nonlinear SMC algorithm within the framework of MPC
3. Realization of drug dosage limitation for simulation of the system
4. Consideration of realistic initial values for the simulation of the overall feedback system

5. Performance validation of novel sigmoid-SMC based MPC optimizer using both proposed (single-input) and multi-input minimal HIV immune system dynamical model.

2. Materials

This study employs a mathematical framework to minimize HIV viral load and analyze the impact of protease inhibitors on HIV dynamics as well as human immune system, using ART. This section underlines the materials and structure, such as system state variables utilized by mathematical model, control variables, system constants and parameters, and lastly, research objectives, which are integral for the formulation of proposed control methodology and algorithm design.

2.1. ***Mathematical Framework***

An ordinary differential equation (ODE) based mathematical model is utilized by this research work to describe the interaction of HIV particles with healthy CD4+ T cells. The mathematical dynamics also encapsulates the response of human body's natural immune system and the administered proetase inhibitor, to the presence and activity of HIV. As the proposed algorithm is employed for two mathematical systems having single and three control inputs respectively, the following state variables of proposed and considered system models are utilized in this research study:

- x_1 (and x): Represents healthy CD4+ T cells that are attacked by the HIV particles for their replication process.
- x_2 (and y): Represents infected CD4+ T cells that produce the virus copies after infection by the HIV.
- x_3: Cyto-toxic T lymphocyte precursors that initiates the immune system response in an event of virus attack.
- x_4: Cyto-toxic T lymphocyte effectors that destroy the infected CD4+T cells to hamper HIV replication.
- x_5 (and v): Represents the dynamics of HIV particles.
- x_6: Represents the inactive HIV particles, that are unable to infect due to the successful action of protease inhibitors.

Control Input: The proposed nonlinear HIV dynamical system employs protease inhibitor as control input to indirectly curb HIV proliferation by preventing the HIV particles to replicate themselves. However, as discussed earlier in section 1, to prove the flexibility of proposed control algorithm, it is also designed based on three-state and three-input minimal HIV dynamical system. For the three-input minimal HIV dynamical model, fusion inhibitor, reverse transcriptase inhibitor, and protease inhibitor are represented as three separate control inputs. These inputs are modeled independently to examine the ability of the proposed nonlinear control framework to regulate multiple drug-action pathways simultaneously within the mathematical model. The independent-input formulation provides flexibility for evaluating the contribution of each control channel; however, it does not impose the clinical requirement that combination therapy components be administered according to a fixed or coordinated treatment regimen. The mathematical model constituting the above mentioned state variables, along with the impact of control input(s) provides the basis for design of proposed algorithm. Thus, by exploiting this complex mathematical foundation, the multifaceted objective of ART (and cART), toxicity minimization and health sustenance can be attained in simulation environment.

2.2. ***Incorporated Dynamics***

To get a better understanding of the system process, following dynamics are considered:

- Protease inhibition dynamics: Protease inhibitors break the reproduction cycle of the HIV. These drugs bind themselves with the freshly produced virus copies and prevent them from maturing into infection causing virus particles by blocking the enzyme protease. This study incorporates this functionality of protease inhibitors in detail and thus propose separate dynamics for mature and immature virus particles.

- Immune system dynamics: To effectively manage HIV infection, the model incorporates the human immune system's natural response against disease proliferation.

- Toxicity minimization and impact of protease inhibitor on health: Since protease inhibitors are very toxic, thus, this study develops a multi-objective optimization and nonlinear control based approach to minimize drug toxicity and maximize health sustenance by regulating the administered control input.

2.3. ***System Parameters***

The key system parameters and constants utilized by the HIV dynamical model includes:

- Growth rates:
    1. λ (and λ_3): Production rate of healthy CD4+T cells.
    2. c: Growth rate of CTLP.
    3. q: Rate of differentiation of CTLP into CTLE.
    4. k (and k_3): Rate of production of virus copies from infected CD4+ T Cells.
    5. λ_y: Contribution of reservoir to actively infected CD4+ T cells.
- Killing rates:
    1. r (and r_3): Rate at which healthy cells are infected by virus.
    2. ρ: Rate at which CTLEs destroy infected cells.
- Infection Rate and Drug Impacts:
    1. r: Rate of infection of CD4+ T cells.
    2. k_v: Drug efficacy.
- Decay rates:
    1. d (and d_3): Natural death of healthy CD4+T Cells
    2. a (and a_3): Natural death of infected CD4+T Cells
    3. b: Decay rate of CTLP.
    4. h: Decay rate of CTLE.
    5. τ (and τ_3): Natural death rate of HIV particles.

The functioning and operation of the proposed system is hence guided by these parameters, which ensure realistic relationship between system states and treatment procedure.

2.4. ***Objectives***

The primary objectives of this study are:

1. Indirect Reduction of HIV: To employ a well-coordinated, multi-objective approach for efficient reduction of HIV particles by breaking their replication process using regulated control input.
2. Side effect reduction: Administration of optimized treatment dosages, and thus indirect reduction of treatment burden.
3. Health Sustenance: Maximization of healthy CD4+ T cell population and indirect minimization of infected CD4+ T cell population.
4. Evaluating cART using a multi-input HIV model: To assess the flexibility of the proposed nonlinear control framework using a three-state, three-input HIV model in which FI, RTI, and PI are represented as separate control channels.

Thus, by minimizing HIV particles and infected CD4+ T cell population, the overall infection can be reduced, while ensuring health sustenance. Similarly, by robustly managing the drug dosage, anti-viral therapy against HIV can be carried out while reducing the treatment burden indirectly through efficient and effective dosage management in simulation framework.

3. Methods

A detailed description of the proposed control strategy, system dynamics, controller derivation, stability analysis and simulation framework is provided in this section. The employed methods and strategies aim to realize the objectives of this research study study through a novel combination and hybridization of advanced nonlinear control technique and practical implementation methods.

3.1. ***Dynamical Single-Input Nonlinear Model***

Previous attempts to control drug injection for anti-retro-viral therapy utilizes either a minimal model that poorly represents the dynamics of the human body or a model that incorporates drug dosage in the form of drug effectiveness. This study considers a model that not only includes the affect of CTLEs against viral load, but it also considers both drug dosage and effectiveness to better understand the drug action against viral load. The model utilized in this study is represented by eq.(1) and is depicted in fig.(1).

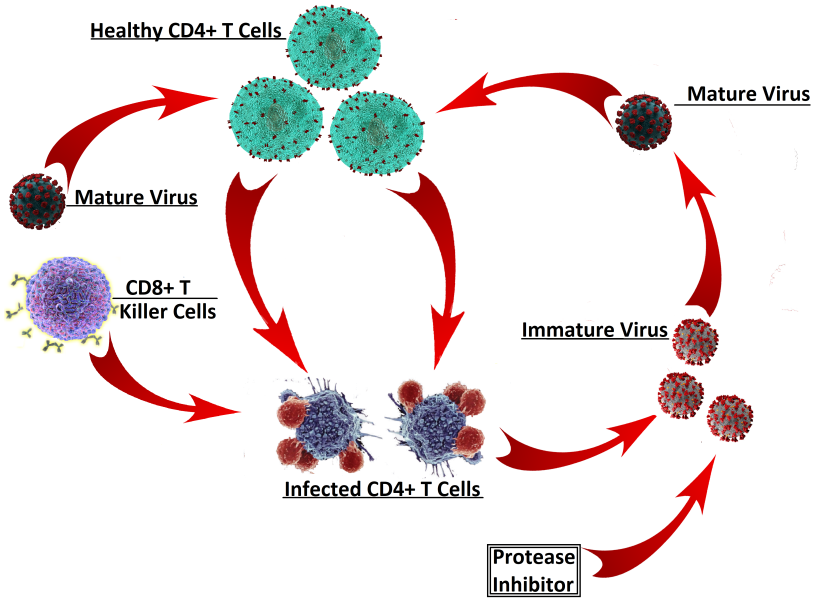


Figure 1: Interaction between HIV - CD4+T - CD8+T (killer) and Proetase Inhibitor

$$\begin{cases} \dot{x}_1 = \lambda - dx_1 - rx_1x_5 \\ \dot{x}_2 = rx_1x_5 - ax_2 - \rho x_2x_4 \\ \dot{x}_3 = cx_1x_2x_3 - cqx_2x_3 - bx_3 \\ \dot{x}_4 = cqx_2x_3 - hx_4 \\ \dot{x}_5 = kx_2 - \tau x_5 - uk_vx_5 \\ \dot{x}_6 = uk_vx_5 - \tau x_6 \end{cases} \tag{1}$$

All the constants in eq.(1), along with the units of measurement are presented in tab.(1) and these parameter values have been sourced from Ref. [22] and [25].

The dynamics of the healthy CD4+ T cells are represented by the state x_1. These cells are produced at a constant rate λ and they die at a rate dx_1. Whereas, they are infected by mature virus particles (x_5) at the rate of rx_1x_5. The parameter "r" represents the rate of infection of healthy CD4 T cells. Its value directly represents the aggression of the HIV infection being caused by the virus. In this study, to test the robustness and efficiency of the proposed algorithm, this infection rate value is kept significantly higher than standard clinical estimates. This is a deliberate

Table 1: Parameters of Dynamical HIV - Lymphocytes Nonlinear Model

Parameter	Units & Value
λ	$7cell\ \mu l^{-1}\ day^{-1}$
d	$7 \times 10^{-3} day^{-1}$
r	$5 \times 10^{-2} day^{-1}$
a	$0.0999\ day^{-1}$
ρ	$2\ \mu l\ cells^{-1}\ day^{-1}$
c	$5 \times 10^{-6}\ \mu l^2\ cells^{-2}\ day^{-1}$
q	$5 \times 10^{-6}\ \mu l\ cells^{-1}\ day^{-1}$
b	$0.017\ day^{-1}$
h	$0.06\ day^{-1}$
k	$300\ copies\ ml^{-1} cells^{-1} \mu l day^{-1}$
τ	$0.2\ day^{-1}$
k_v	0.5

choice to simulate an extreme infection scenario, so that the proposed control algorithm may be tested under more challenging conditions.

Similarly, the state x_2 represents the infected CD4+ T cells. These infected variants of CD4+ T cells are produced due to the infection of mature virus particles at the rate rx_1x_5 and they die either naturally at the rate ax_2 or are taken care of by the Cyto-Toxic T-Lymphocyte (CTL) effectors, called CTLEs (x_4) at the rate $\rho x_2 x_4$. The Cyto-Toxic T-Lymphocyte cells can be categorized as two different type of cells; activated and non-activated, that makes the CTLE pool. These are named as CTL effectors (CTLEs) and CTL precursors CTLP (x_3). The CTLp are produced at a rate depending on $cx_1x_2x_3$ and die at a rate of bx_3. When the CTL precursors receive cytokine signals, they become activated against the infected cells and hence, they differentiate into CTLEs at the rate cqx_2x_3. The CTLEs die at the rate hx_4.

The term x_5 represents the dynamics of mature virus particles, that are the main culprit in HIV infection progression. These free virus are produced by the infected CD4+ T cells and are cleared

naturally at the rate τx_5. However, as per the current advancements in medicine, it is not possible to kill the HIV using any drug. The term u represents the injected drug i.e. the protease inhibitor, that affect the newly produced virus copies by inhibiting the production of protease and thus rendering such virus particles non-infectious. Not every molecule of drug is able to react and affect the viruses. In-fact, only a percentage of the drug dosage is able to effectively inhibit the protease production in virus particles. This drug characteristic is modeled through the introduction of a constant, k_v, representing the drug efficiency. Lastly, the immature non-infectious virus particles, that remain non-infectious as a result of drug action. These virus particles are represented by x_6. The virus copies are unable to replicate themselves due to the binding of protease inhibitor with them. These non-infectious HIV particles then die naturally at the rate τx_6.

3.2. ***Dynamical Multi-Input Minimal Nonlinear Model***

One of the main objective of carrying out this research study is to devise a control strategy that is flexible enough to work in a number of different conditions. The effectiveness and performance of the proposed control system should be equally potent against HIV when multiple inputs are considered. Similarly, the parameters for any HIV-Immune system dynamical model reflect the conditions of patient under consideration. The controller must be tested for its performance when a different set of system parameters are employed. Thus to validate the effectiveness of designed algorithm, its performance is validated against a three-input minimal model with experimentally derived system parameter values, provided in Ref. . The minimal model utilized for this is presented in eq.(2). Whereas, the system parameters considered for eq.(2), which are presented in Ref. [35], are provided in tab.(2).

$$\begin{cases} \dot{x} = \lambda_3 - d_3 x - r_3 x v (1 - u_{fi}) \\ \dot{y} = r_3 x v (1 - u_{fi})(1 - u_{ti}) - a_3 y + \lambda_y \\ \dot{v} = k_3 y (1 - u_{pi}) - \tau_3 v \end{cases} \tag{2}$$

The state x represents the dynamics of healthy CD4+ T cells, whereas, dynamics of infected CD4+ T cells and HIV are represented by states y and v respectively. Healthy CD4+ T cells are produced at a rate λ_3 and they die at the rate $d_3 x_1$. HIV infects the healthy CD4+ T cells at the rate of $r x_1 x_5$. As explained earlier in section 1, the HIV particles have to fuse on the surface of T cells to infect them. Thus, by employing fusion inhibitors (represented as u_{fi}), this rate of infection can be

Table 2: Parameters of Minimal Dynamical HIV Nonlinear Model

Parameter	Units & Value
λ_3	300 $cells\ \mu l^{-1}\ day^{-1}$
d_3	0.18 day^{-1}
r_3	$3.9 \times 10^{-6}\ ml\ copies^{-1}\ day^{-1}$
a_3	1 day^{-1}
λ_y	$2 \times 10^{-6}\ cells\ \mu l^{-1}\ day^{-1}$
k_3	5900 $copies\ \mu l\ cells^{-1}\ ml^{-1}\ day^{-1}$
τ_3	18.8 day^{-1}

reduced to indirectly thwart the infectious attack of HIV. Similarly, reverse transcriptase inhibitors have been employed to stop the reverse transcriptase process, that is responsible for producing the replicas of HIV using the infected CD4+ T cell as its host. The control input u_{ti} represents the action of reverse transcriptase inhibitors on the dynamics of infected CD4+ T cells. $a_3 y$ represent the death rate of state y, whereas, λ_y represents the additional contribution of infected CD4+ T cells from all reservoir processes that produce virus copies. The HIV particles replicate themselves using infected CD4+ T cells at the rate $k_3 y$. The control input u_{pi} represent protease inhibitors that belong to another class of drug, which impact newly produced copies of HIV which haven't matured yet, and render such virus particles ineffective against CD4+ T cells. Lastly, the virus particles die at the rate $\tau_3 v$. This minimal model of HIV dynamics does not include the impact CTLE and CTLP.

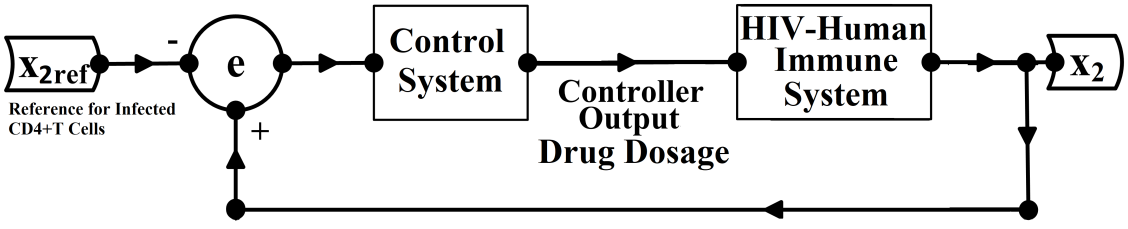


Figure 2: Close Loop Control

3.3. ***Proposed Control Methodology***

An indirect approach is proposed in this study to manage the viral load in an HIV infected person through anti-retro viral therapy. As stated earlier in section 1, there is currently no medicine or drug available to directly kill the HIV virus. The drugs presently employed for ART and cART, affect the reproduction or life cycle of the virus to stop the infection from progression. The protease inhibitors affect the freshly created virus copies and impedes their growth process, rendering them ineffective to spread infection to healthy CD4+T cells. Similarly, fusion inhibitors latch themselves to the sites on the surface of CD4+ T cells where the HIV particles are supposed to latch, thus indirectly blocking their access to the healthy cell. Whereas, reverse transcriptase inhibitors restrain the replication process within an infected CD4+ T cell to directly impact the reproduction or replication cycle of the HIV. Hence, these drugs resist the HIV proliferation such that they die and are cleared naturally from the body. Thus, steadily reducing the viral load and infection progression in human body. As discussed earlier in section 1 and 2, the approach utilized for HIV minimization in this research study is based on the design of nonlinear controllers that considers the minimization of infected CD4+T cells to indirectly but ultimately limit HIV proliferation. The generalized approach opted for the implementation of anti-HIV therapy is depicted in fig.(2). The control system requires the information of state variables to compute the drug dosage required for effective and optimized reduction of HIV viral load, along with maximization of healthy CD4 count. By doing so, the HIV disease progression can be seriously hampered, as the viral copies are produced by these infected CD4+T cells.

This study considers a model that not only includes the affect of CTLEs against viral load, but it also considers both drug dosage and effectiveness to better understand the drug action against viral load. The CTLEs are the human body's natural response against the infected cells that are spreading disease inside. These cells are hence, also termed as "killer cells", as they are responsible for the killing and disposition of infected CD4+T cells. Similarly, this research work also considers another model that incorporates both fusion and reverse transcriptase inhibitors alongside protease inhibitors to curb the advancements of HIV infection. Thus, this study proposes both ART and cART against HIV infection by controlling the amount of anti-HIV drugs, administered to the infected person, according to the underlying situation of disease progression. Hence, this research work suggests that the dosage should increase or decrease accordingly, as per the real time status of infection. The general process to control the drug dosage in an infected person undergoing anti-HIV

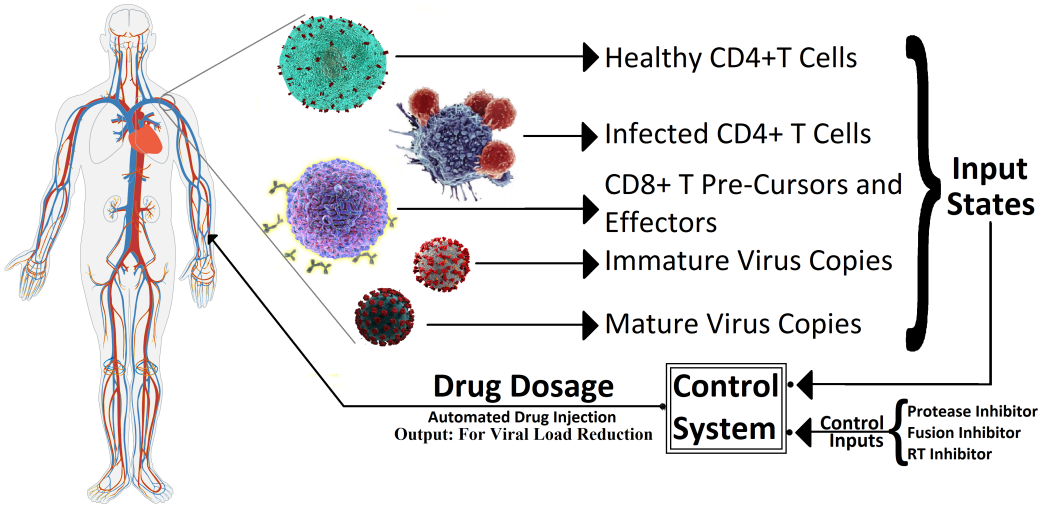


Figure 3: Drug Dosage Adjustment for ART against HIV Infection

therapy is represented in fig.(3).

The proposed algorithm upgrades conventional sliding mode controller by incorporating the sigmoid function based switching control. This nonlinear control system can be generally realized by fig.(2). Yet this integration of sigmoid function with SMC can only perform one objective at a time. However, it is pertinent to maximize CD4 count and minimize treatment induced side effects along with minimization of viral load. Thus a multi-objective approach such as MPC is necessary to fulfill all of these objectives. Hence, to exploit both robustness of SMC and multi-objective approach of MPC, a mechanism is opted in this research study to combine both of these control techniques. The proposed MPC algorithm is depicted in fig.(4). The time horizon (mentioned as "Th" in fig.(4)) refers to the total time of therapy, i.e. the duration until which the control inputs are optimized. Whereas, the prediction horizon, (mentioned as "Ph" in fig.(4)) refers to the time duration, over which the system states are predicted and the control inputs are optimized via cost minimization. In order to completely integrate SMC within MPC structure, several pair of controller gains are also considered so that based on current system situation, best possible controller gains may be selected to optimize computed control inputs. The proposed algorithm can be summarized in the following steps:

1. Initialization of the algorithm using initial values of the states
2. Calculation of control inputs on the basis of previous state values and considered controller

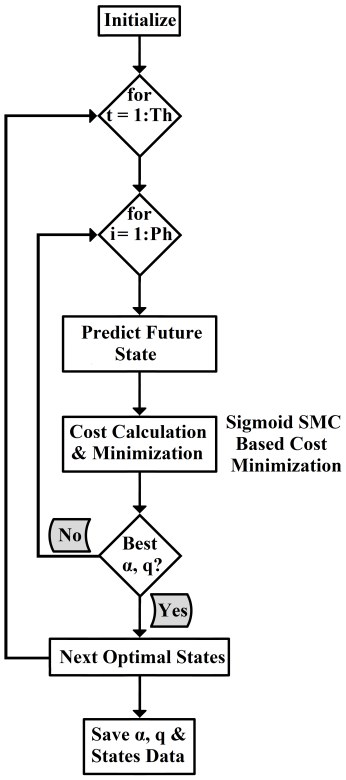


Figure 4: MPC

gains via SMC

3. Prediction of the next state values on the basis of the optimized control input values
4. Cost estimation using the objective function.
5. Selection of best control inputs and controller gains on the basis of the best estimated cost throughout the considered horizon
6. t = t+1 (increment of the time instant)
7. Repeat this algorithm again from step 2

3.4. ***Control Objectives***

As discussed in Section 1, recent studies mainly focused on immediate reduction of HIV viral load, while neglecting the problem of over dosage and the harmful side effects of anti-retro-viral

drugs. The control objectives considered in this study for the design of anti-HIV algorithm are following:

1. CD4+ T Cell Maximization: A healthy CD4+ T cell count is of prime importance, as these cells are necessary to monitor opportunistic diseases and infections.
2. Viral Load Reduction: An increased viral load implies more advanced stage of HIV infection besides patient's deteriorated CD4+ T count and general health condition.
3. Control Input Minimization: As administered dosage of anti-HIV drugs can have severe side effects on general health and well-being of the patient, thus it is intended to minimize control inputs to prioritize health sustenance.

3.5. ***Design of Proposed SMC based MPC***

Since, the virus particles are very small and hard to detect, the condition of infection progression in a patient and the subsequent drug dosage is determined using healthy and infected CD4+T cell count. The nonlinear sigmoid SMC-based MPC algorithm is designed in this section, with the goal to minimize the infected CD4+T cell population. This is in turn achieved indirectly by injecting protease inhibitors to combat HIV particles. Thus, by limiting the production of virus copies, the viral load is reduced.

Owing to its numerous advantages over traditional nonlinear algorithms, SMC is generally more desirable. Robustness, ability to cater for nonlinearities effectively, and simplicity of design and implementation makes SMC very efficient. Yet, due to its inherent nature of operation, the controller introduce chattering in system's response [36, 37]. These transients especially become problematic for applications such as drug regulation, which require very precise regulation and control. Rapid oscillations in drug dosage can not only result in administration of increased treatment dosage levels but it will also introduce transients in system states causing further inconvenience and even harm to the patient under consideration. Thus, a sigmoid based smoothing function is incorporated into the framework of SMC to smooth out its inherent chattering problem.

3.5.1. ***Design of Smooth SMC using Three-input HIV System Dynamics***

This section presents the design and derivation of proposed smooth SMC algorithm based on the mathematical system presented in eq.1. Let e be the error term defined as the error between

the actual and desired number of infected CD4+ T cells. As the latter is 0, thus:

$$e = x_2 - 0 \tag{3}$$

Consider the following sliding surface and its derivative:

$$S = K_1 e + K_2 x_5 \tag{4}$$

or

$$S = K_1 x_2 + K_2 x_5 \tag{5}$$

taking time derivative of eq.5, we get:

$$\dot{S} = K_1 \dot{x}_2 + K_2 \dot{x}_5 \tag{6}$$

where, K_1 and K_2 are positive constants. To bring the system trajectory to the sliding surfaces and then to keep it there all the time, let:

$$\dot{S} = K_1 \dot{x}_2 + K_2 \dot{x}_5 = \frac{-K_s S}{1 + e^{-\phi S}} \tag{7}$$

where, K_s is a positive definite design constant. The parameter ϕ reflects the steepness of the sigmoid function; the greater the value of ϕ is, the steeper the sigmoid function. Now, to analyze the stability of the system, consider the following Lyapunov candidate functions:

$$V = \frac{1}{2} S^2 \tag{8}$$

By taking the time derivative of eq.(8):

$$\dot{V} = S\dot{S} = -S(\frac{K_s S}{1 + e^{-\phi S}}) \tag{9}$$

Hence, eq.(9) can be written as:

$$\dot{V}_1 = S\dot{S} = -(\frac{k(S)^2}{1 + e^{-\phi S}}) \tag{10}$$

As, K_s is a positive constant, and $1/(1 + e^{-x}) \geq 0$, for all values of x, $\dot{V}$ is negative definite, which ensures that the error stably converges to 0 with in finite time.

The control input can be computed using eq.(7):

$$u = K_1 \frac{r x_1 x_5 - a x_2 - \rho x_2 x_4}{K_2 K_v x_5} + \frac{k x_2 - \tau x_5}{K_v x_5} + \frac{K_s S}{K_2 K_v x_5 (1 + e^{-\phi S})} \tag{11}$$

The term $\frac{K_s S}{K_2 K_v x_5(1+e^{-\phi S})}$ in eq.(11) is the sigmoid based switching control input for u, whereas the remaining terms are collectively called the equivalent control. Owing to these soft switching input terms, the proposed SMC controller is expected to produce almost negligible oscillations in the dynamics of system states.

3.5.2. ***Design of Smooth SMC using Three-Input HIV System Dynamics***

This section presents the design and derivation of proposed multi-input smooth SMC algorithm based on the mathematical system presented in eq.2. As the considered dynamics incorporate the impact of three different classes of drugs or control inputs, thus three different control laws are required for each respective control input. Let us define two error terms e_x and e_y representing the error between actual and desired healthy CD4+ T cells (e_x) and infected CD4+ T cells (e_y). The desired value of infected CD4+ T cells is 0, whereas, the desired healthy CD4+ T cells value can be find by considering steady state conditions (when state v becomes 0), thus:

$$e_x = x - x_d = x - \frac{\lambda_3}{d_3} \tag{12}$$

$$e_y = y - y_d = y - 0 \tag{13}$$

Since the system has multiple control inputs, three different sliding surfaces are considered here to compute the control inputs u_{fi}, u_{ti} and u_{pi}. Consider the following sliding surfaces and their derivatives:

$$S_f = K_x e_x \tag{14}$$

$$S_t = K_y e_y = K_y y \tag{15}$$

$$S_p = K_{p1} e_y + K_{p2} v = K_{p1} y + K_{p2} v \tag{16}$$

where, K_x, K_y, K_{p1} and K_{p2} are positive constants. Taking time derivative of eq.14, eq.15 and eq.16 , we get:

$$\dot{S_f} = K_x \dot{x} \tag{17}$$

$$\dot{S}_t = K_y \dot{y} \tag{18}$$

$$\dot{S}_p = K_{p1} \dot{y} + K_{p2} \dot{v} \tag{19}$$

To bring the system trajectory to the sliding surfaces and then to keep it there all the time, let:

$$\dot{S}_f = K_x \dot{x} = \frac{-K_f S_f}{1 + e^{-\phi S_f}} \tag{20}$$

$$\dot{S}_t = K_y \dot{y} = \frac{-K_t S_t}{1 + e^{-\phi S_t}} \tag{21}$$

$$\dot{S}_p = K_{p1} \dot{y} + K_{p2} \dot{v} = \frac{-K_p S_p}{1 + e^{-\phi S_p}} \tag{22}$$

where, K_f, K_t and K_p are positive definite design constants. The parameter ϕ reflects the steepness of the sigmoid function; the greater the value of ϕ is, the steeper is the sigmoid function. Now, to analyze the stability of overall system, consider the following Lyapunov candidate functions:

$$V_f = \frac{1}{2} {S_f}^2 \tag{23}$$

$$V_t = \frac{1}{2} {S_t}^2 \tag{24}$$

$$V_p = \frac{1}{2} {S_p}^2 \tag{25}$$

By taking the time derivative of eq.(23), (24) and (25), we get:

$$\dot{V}_f = S_f \dot{S}_f = -S_f \left(\frac{K_f S_f}{1 + e^{-\phi S_f}}\right) = -\left(\frac{K_f (S)_f^2}{1 + e^{-\phi S_f}}\right) \tag{26}$$

$$\dot{V}_t = S_t \dot{S}_t = -S_t \left(\frac{K_t S_t}{1 + e^{-\phi S_t}}\right) = -\left(\frac{K_t (S)_t^2}{1 + e^{-\phi S_t}}\right) \tag{27}$$

$$\dot{V}_p = S_p \dot{S}_p = -S_p \left(\frac{K_p S_p}{1 + e^{-\phi S_p}}\right) = -\left(\frac{K_p (S)_p^2}{1 + e^{-\phi S_p}}\right) \tag{28}$$

As, K_f, K_t and K_p are positive constants, and $1/(1 + e^{-\theta}) \geq 0$, for all values of θ, proving $\dot{V}_f$, $\dot{V}_t$ and $\dot{V}_p$ to be negative definite, which ensures that the error stably converges to 0 with in finite time.

Now, eq.(20), (21) and (22) can be utilized to compute the final control laws for $u_f i$, $u_t i$ and $u_p i$, given by:

$$u_{fi} = [-\frac{K_f S_f}{1 + e^{-\phi S_f}} - K_x(\lambda_3 - d_3 x - r_3 xv)]\frac{1}{K_x r_3 xv} \tag{29}$$

$$u_{ti} = [\frac{K_t S_t}{1 + e^{-\phi S_t}} + K_y(r_3 xv(1 - u_{fi}) - a_3 y + \lambda_y)]\frac{1}{K_y r_3 xv} \tag{30}$$

$$u_{pi} = [\frac{K_p S_p}{1 + e^{-\phi S_p}} - K_{p2}\tau_3 v + K_{p2} k_3 y + K_{p1}\dot{y}]\frac{1}{K_{p2} k_3 y} \tag{31}$$

Once again, the terms $\frac{K_f S_f}{1+e^{-\phi S_f}}$, $\frac{K_t S_t}{1+e^{-\phi S_t}}$ and $\frac{K_p S_p}{1+e^{-\phi S_p}}$ in eq.(29), eq.(30) and eq.(31) are sigmoid based switching control inputs, whereas the remaining terms are collectively called the equivalent control. It should be noted that the three control inputs (u_{fi}), (u_{ti}), and (u_{pi}) are treated as independent control channels in the mathematical formulation. Accordingly, the proposed controller optimizes their magnitudes independently according to the system states and the adopted objective function. The three-input formulation is therefore intended to represent the distinct mechanisms through which different anti-retro-viral drug classes influence HIV dynamics, rather than to prescribe a clinical dosing schedule or a sequential drug-administration strategy. In an actual cART regimen, the timing, dosage, pharmacokinetics, adherence, drug-drug interactions, and regimen composition would need to be constrained according to established clinical protocols. These considerations are outside the scope of the present mathematical model.

Moreover, although (u_{fi}), (u_{ti}), and (u_{pi}) are computed and updated in parallel by the controller, this should not be interpreted as a sequence in which the effect of one treatment is assumed to terminate before another treatment is applied. The three inputs are evaluated at the same control instant and represent the independently regulated contributions of the corresponding drug-action pathways to the HIV dynamical model. Once these inputs influence the system, their effects are reflected through the subsequent state evolution of the model and are therefore not interpreted as instantaneously disappearing when the control inputs are updated at the next sampling instant. Accordingly, the different magnitudes of the three control trajectories indicate the controller's instantaneous allocation of treatment intensity among the modeled drug-action pathways rather than a prescription for sequential drug administration. Nevertheless, the present model does not explicitly include pharmacokinetic or pharmacodynamic compartments describing drug concentration, absorption, clearance, or persistence. Therefore, the persistence of therapeutic effects

is represented only through the adopted dynamical equations and should not be interpreted as a quantitative pharmacological representation of drug residence time.

3.5.3. ***MPC Framework***

The designed sigmoid SMC-based nonlinear controllers presented in subsections 3.5.1 and 3.5.2 are incorporated within the framework of MPC to exploit the advantages of both the techniques. MPC is an optimization based, system dependent algorithm that computes the best possible control input, among the candidate control inputs, after analyzing and predicting the future states of the system depending on the cost function [38]. Hence, the three fundamental components of MPC are system dynamics, objective function and minimization algorithm [39, 31]. However, the proposed algorithm is designed without linearizing the nonlinear system equations, as mentioned in eq.(1) and eq.(2).

The objective function employed in this study, not only focuses on reduction in viral load, but also considers the drug dosages so that the negative impact of anti-HIV therapy maybe minimized as much as possible. Similarly, the cost function also includes the impact of the treatment therapy on healthy CD4+T cells as it can directly indicate the state of health of the patient. The cost function ($J(t)$) considered for the single-input HIV dynamical model presented in eq.(1), is mentioned below in eq.(32). Similarly, the cost function considered for three-input dynamical model presented in eq.(2) is presented below in eq.(33). Since this model incorporates three different control inputs, thus the cost function presented in eq.(33) includes two extra terms representing the control inputs for fusion inhibitor and and reverse transcriptase inhibitor.

$$J_1(t) = w_1 \times (x_1 - x_{1ref})^2 + w_2 \times {x_5}^2 + w_3 \times u^2 \tag{32}$$

$$J_3(t) = w_4 \times (x_1 - x_{1ref})^2 + w_5 \times {x_5}^2 + w_6 \times ({u_{fi}}^2 + {u_{ti}}^2 + {u_{pi}}^2) \tag{33}$$

where, w_1, w_2, w_3, w_4, w_5 and w_6 are the positive valued design constants representing weights of each term present in above mentioned cost or objective functions.

3.6. ***Drug Dosage***

In recent time, numerous protease inhibitors have been employed to curb the advancement of HIV infection. Currently, for example, the Food and Drug Administration department of the United States recommend 11 protease inhibitors for HIV [40]. As stated earlier, these drugs are

very toxic and have adverse affects on the health of individuals [16, 41]. To analyze the amount of molecules injected in a patients blood stream per day, the dosage of protease inhibitor: Atazanavir is considered. The maximum daily dosage for treatment-naive patients (a patient who has never taken any ART drug) is 400 mg per day [42, 43]. Since, the molar mass of Atazanavir is 704.9 grams per mole, hence a 400 mg per day dosage corresponds to 3.416×10^{20} molecules per day [44]. Since an adult human body consists approximately 5 liters of blood, hence, the amount of molecules present in 1 μliter of blood stream per day can be found out to be 6.8326×10^{13}. Thus, the maximum allowed dosage that can be given to the system in close-loop nonlinear feedback control is 6.8326×10^{13} molecules $\mu l^{-1}\ day^{-1}$.

4. Simulation & Results

The performance of the proposed multi-objective sigmoid SMC-based MPC algorithm is evaluated in this section. The controller has been designed based on the ODE mathematical model of interaction of HIV-human immune system, presented in eq.(1) and eq.(2).

4.1. ***Simulation Setup***

The simulations are performed considering two different initial values of Healthy CD4+T cells as well as viral load. These initial conditions hence, imitate the condition of patients in two different stages of HIV progression, i.e. stage 1 and 2 of HIV. For stage 1, the initial value for CD4+T cell count is considered to be 700 $cells\mu l^{-1}$, whereas the initial viral load is set at 300 $copies\mu l^{-1}$. Similarly, for stage 2, the initial value of x_1 is set at 350 $cells\mu l^{-1}$ and viral load is set at 10,000 $copies\mu l^{-1}$. These values are set according to the standardized classification of HIV infection based on viral load and CD4 count [2]. Both of these initial conditions are considered while experimenting the proposed algorithm with the system model presented in eq.(1) and eq.(2). For system presented in eq.(1), the initial values for x_2 and x_6 are considered to be 0, whereas, the initial values of x_3 and x_4 are set at 1×10^3 and 1×10^{-7} respectively [45]. Similarly, for model presented in eq.(2), the initial condition for infected CD4+ T cells is considered to be 100 $cells\mu l^{-1}$.

4.1.1. ***Environment***

Simulations for this research work are performed in MATLAB using the proposed sigmoid SMC-based MPC algorithm designed using the non-linear system dynamics presented in eq.(1) and eq.(2).

Table 3: Parameters of Nonlinear Controllers

Parameter	Value	Parameter	Value
Time Horizon	1000	w_4	10
Prediction Horizon	10	w_5	100
w_1	10	w_6	0.01
w_2	100	K_f	1
w_3	0.01	K_t	9
K_s	7000	K_p	1
ϕ	0.01		

4.1.2. ***Controller Design Parameters***

The values of design constants of each evaluated controller, are kept the same for the simulations of both Stage 1 and Stage 2 HIV. The values of these constants are provided in tab.(3). However, the proposed sigmoid SMC-based MPC algorithm has been designed in such a way that the algorithms itself determines the best possible pair of K_1 and K_2 based on the evaluated cost using objective function. The controller, thus selects the best possible values of each of these constants from the following pool: [0.001, 0.01, 0.1, 1, 10, 100]. Hence, the algorithm evaluates the affiliated cost using each possible pair of constants K_1 and K_2 using these values, and based on the results, it determines the best possible combination. Lastly, the simulations were performed while keeping the drug efficacy constant $'k_v'$ at 0.5. That means, only 50% of the drug dosage end up combining and hence hampering HIV's infectiousness.

4.1.3. ***Performance Comparison Framework***

The performance comparison is established based on the following metrics:

- Quantitative Parameters:
    1. Settling Time
    2. Steady State Error
    3. Overshoot

4. Initial and Final Dosage

- Qualitative Parameters:
  1. Viral Growth Trend
  2. Ability of the controller to converge HIV particles to zero
  3. Dosage Trend

4.1.4. ***Bench-marking***

The performance of the proposed algorithm is compared with that of the following linear and nonlinear controllers:

1. Nonlinear statefeedback controller
2. Synergetic controller
3. Backstepping controller
4. PID controller
5. LQR controller

4.2. ***P****erformance during Stage-1 HIV (using HIV dynamics given in eq.(1))*

As far as treatment is concerned, the first stage of HIV infection is the most critical. This stage lasts for only two to four weeks and is distinguished by the rapidly spreading and reproducing virus particles as well as infection. Commencement of ART at this stage is considered to be the most effective against HIV, as the host is still healthy and the body is not yet weakened by the opportunistic diseases. This stage is marked with the rapidly dwindling values of CD4 count. The count for a healthy person averages around 1000 $cells\ \mu l^{-1}$, however, during stage-1 HIV, the CD4 count may fall up to 500 $cells\ \mu l^{-1}$. Hence, to study the disease in stage-1, initial value of x_1 is set at 700 $cells\ \mu l^{-1}$. Similarly, the viral load of 10,000 $copies\ ml^{-1}$, considered to be low for HIV is set as the initial condition for stage-1 HIV.

Fig.(5) depicts the response of system dynamics when proposed sigmoid SMC-based MPC algorithm is utilized for reduction of HIV viral load. The proposed controller not only successfully reduced the viral load effectively, but it also did so very swiftly. Moreover, by analyzing the system curves, it can be further observed that the state trajectories are smooth and transient free. This result is achieved due to the smoothing action of the sigmoid function. In contrast, the state

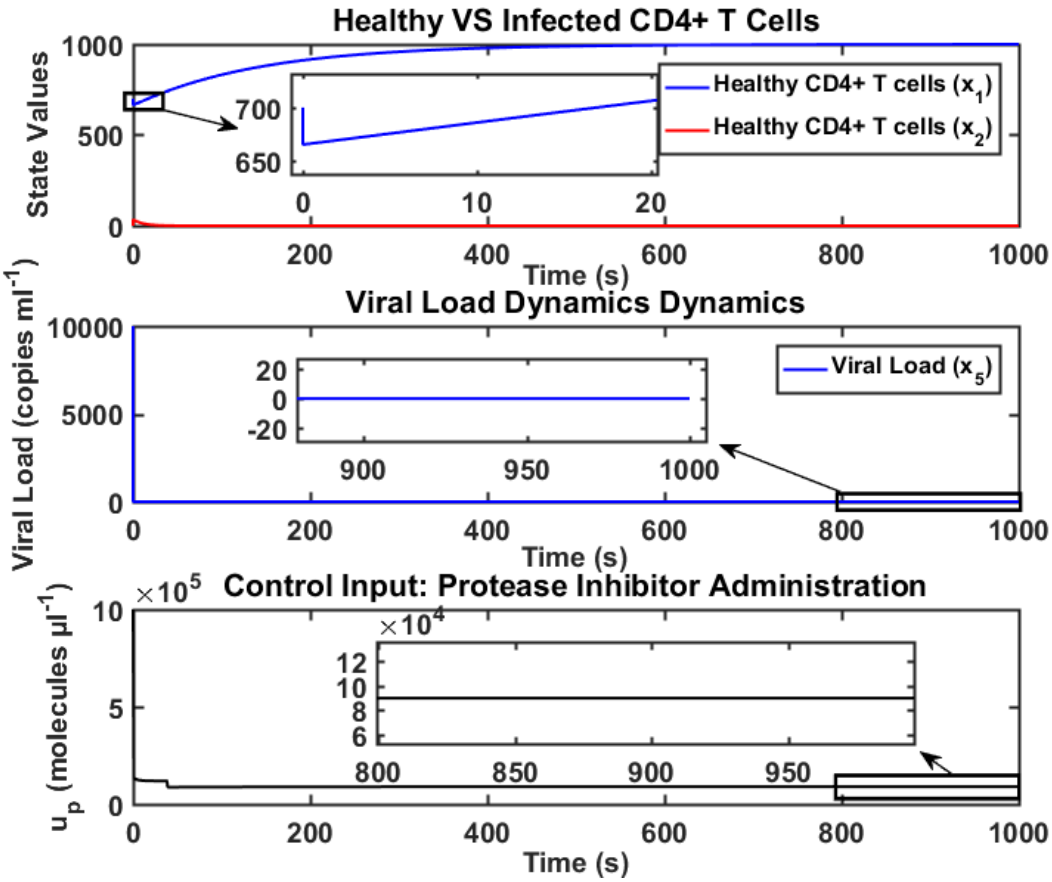


Figure 5: System Dynamics Stage-1 HIV- Proposed Sigmoid SMC-based MPC for Single Input Six State Model

trajectories obtained by using conventional SMC generally depict oscillations and chattering. The dynamics of healthy CD4+ T cells achieved steady state within 400 days. However, an initial drop in healthy cell population is observed as it dropped from 700 to 670 $cells\mu l^{-1}$. The infected CD4+ T cells were also reduced to zero. Whereas, the initial and final dosage administered by the proposed algorithm are 9.9×10^5 $molecules\mu l^{-1}$ and 8.78×10^4 $molecules\mu l^{-1}$ respectively. The detailed performance comparison between the proposed algorithm and the other recently proposed controllers is provided below:

4.2.1. Comparison of Healthy & Infected CD4+T Cells Dynamics

As stated earlier, the healthy amount of CD4+T cells are a direct indication of the patients health and the disease progression. As human body is unable to produce any effective antibodies

against HIV virus, thus, an infected person with high CD4 count is also an easy target for the HIV virus to replicate and multiply. Thus, an affected person under HIV attack, without ART becomes a nesting ground for the viruses. Similarly, a drop in CD4 count also results in an increased infected CD4 cell count. Fig.(6) depicts the response of healthy CD4+T cells undergoing anti-HIV therapy using different feedback controllers.

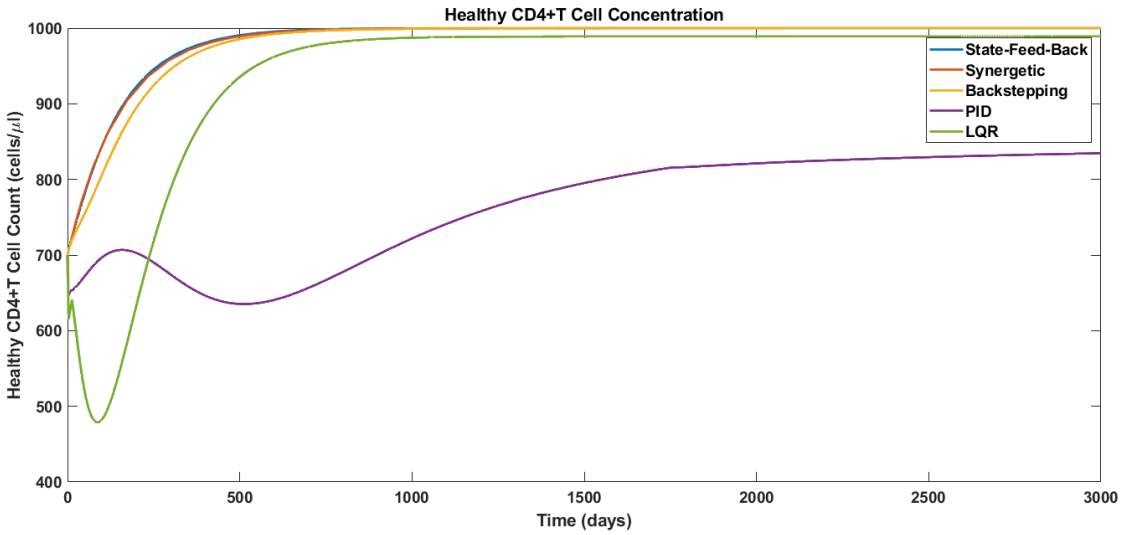


Figure 6: Healthy CD4+T Cell Concentration

As observed from the fig.(6), all the nonlinear controllers performed exceptionally well. The synergetic and state-feedback controllers took more than 500 days to attain steady state, whereas, the backstepping controller took around 550 days to do so. As far as the dynamics of state x_1 is concerned, both the linear controllers performed poorly, especially in comparison with their nonlinear counterparts. Firstly, both the controllers were unable to efficiently administer appropriate drug dosage, resulting in a sluggish response with noticeable steady state differences. Though, the LQR controller exhibited a steep undershoot, it still managed to bring the CD4 count to a healthy level. nevertheless, such a steep decrement in CD4 count may result in detrimental health and well being of the patient. The case of PID is even more complex as the linear controller was unable to cope up with the non-linearities and was very sluggish to administer an appropriate drug dosage and thus, it not only resulted in a drop in the CD4 count, but also depicted a huge steady state error. Thus by comparing fig.(6) with fig.(5), it can be deduced that the proposed sigmoid SMC-based MPC

algorithm achieved steady state much more swiftly in comparison to the other linear and nonlinear controllers.

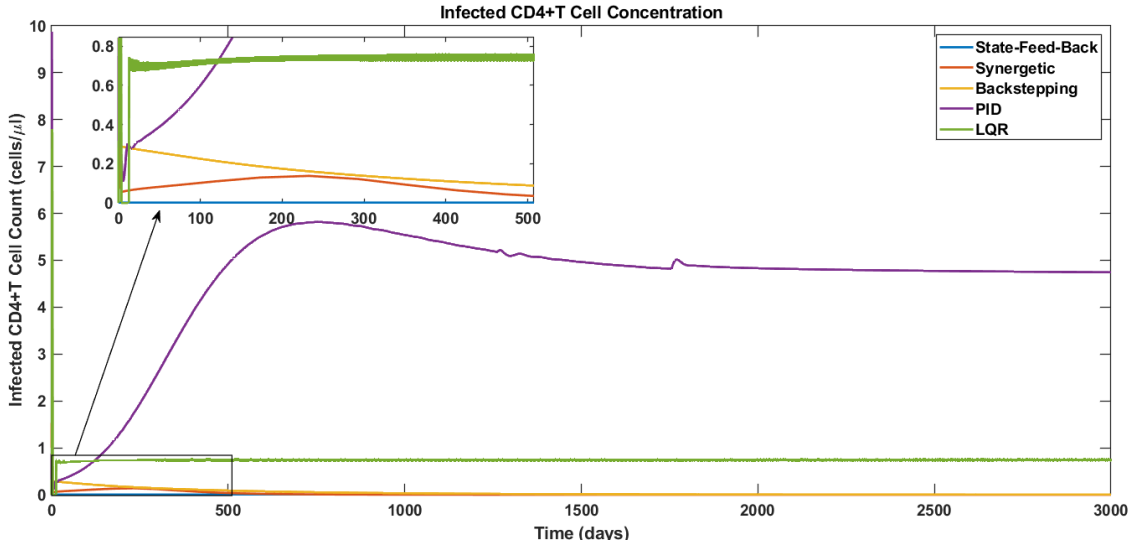


Figure 7: Infected CD4+T Cell Concentration

Fig.(7) depicts the close loop dynamics of infected CD4+T cells. Since the PID and LQR controllers caused a drop in CD4 count, hence, the response of infected CD4+T cells depicted a sharp increase in case of both of these linear controllers. Moreover, both these controllers were unable to completely eradicate the infected CD4 cell populations. Since, the virus particles reproduce using these infected cells, hence, an increase in infected cell population, or sustenance of them results in disease progression and advancement. On the other hand, the nonlinear backstepping and synergetic controllers successfully contain the infection of infected cells and have depicted a continuously reducing trend as well. Although, the synergetic controller did show a slight increase in the infected cell population, yet it exponentially converged all the infected cells to 0. Among the nonlinear controllers, the state-feedback controller is the only one which did not depict a continuously reducing trend of the infected cells, however, it successfully reduced their concentration to a negligible amount of $4.43 \times 10^{-4}\ cells\mu l^{-1}$.

4.2.2. Viral Load Comparison

The response of the viral load observed using recently proposed algorithms is depicted in fig.(8). Although all the controllers improved or atleast sustained the CD4 count, yet the linear controllers

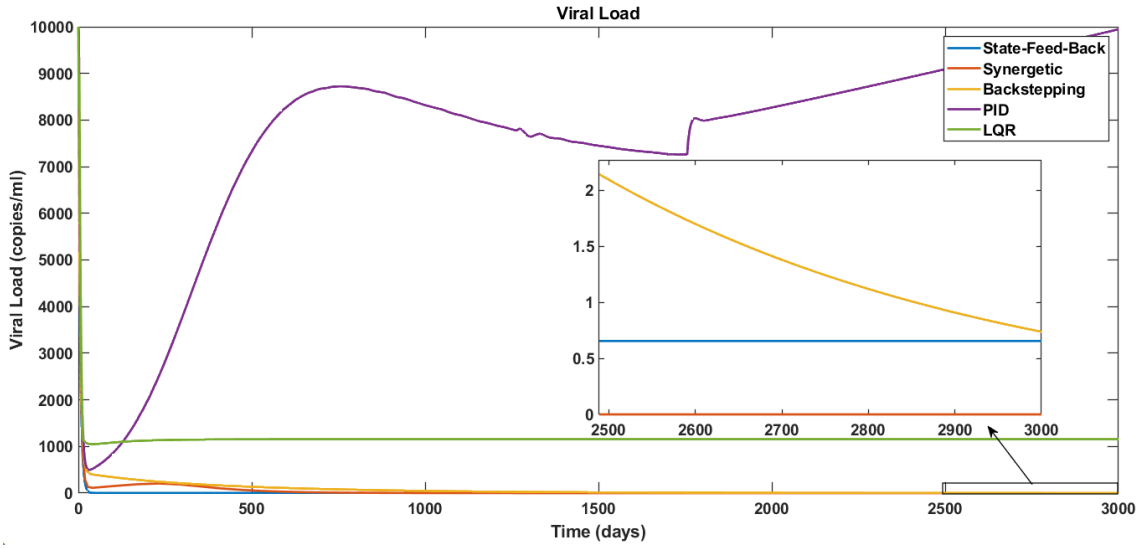


Figure 8: Total Viral Load

performed quite poorly. The LQR controller initially reduced the viral load, yet it failed to completely contain the infection and the viral load converges only upto 1157 $copiesml^{-1}$. The PID remained the worst performing controller, as after initial reduction in viral load, it depicted a continuously increasing trend, indicating deteriorating condition of the infection. Although, the synergetic controller successfully reduced the viral load, yet a small peak can be observed in its response, depicting a sudden rise of 111 $copiesml^{-1}$. The convergence pattern of synergetic controller is faster than that of backstepping controller. State-feed-back and backstepping controller adjusted the drug dosage appropriately to curb any increment in viral load, however, the former converges the viral load up to 0.7 $copiesml^{-1}$ and shows a very slow converging trend towards zero. Hence, it seems as if the state-feedback controller reduces the viral load but does not completely diminish the infectious particles. In comparison, the

*4.2.3. **D**rug Dosage Comparison*

The drug dosage administered by different recently proposed controllers is shown in fig.(9). The initial and final (steady state) dosage, along with the settling time to reach the steady state drug dosage value are the important insights from these drug dosage curves. Initial dosage not only depends on the condition of he patient (i.e. the values of the state variables) but also on the type of controller and its characteristics.

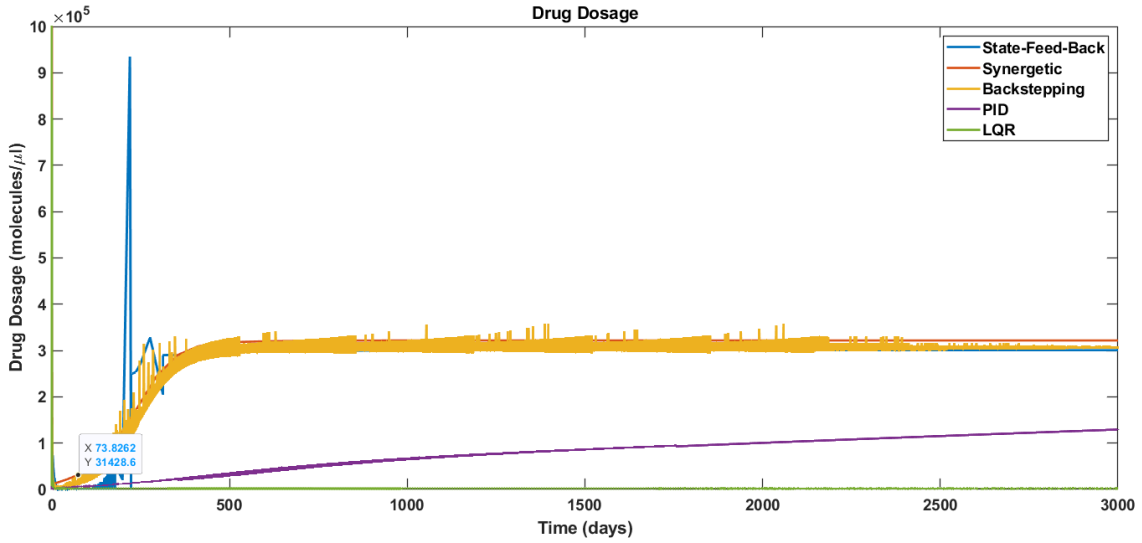


Figure 9: Control Input - Drug Dosage

It can be inferred from fig.(9) that the linear PID controller is overall slow to respond and depicted a continuously increasing drug dosage trend. THe LQR controller was swift to respond, however, it caused the dosage to settle at a much lower value in comparison to the other controllers. If the viral load curve of the the LQR controller depicted in fig.(8) is considered, then it can be concluded that the drug dosage must increase to curb the spread of infection. Yet the LQR depicted a stable trend after settling to its final value without further reducing the viral load.

The nonlinear state-feedback controller depicted the highest initial drug dosage value of 1.6×10^9 $molecules\mu l^{-1}$. A peak value of 9.35×10^5 $molecules\mu l^{-1}$ can also be observed in the dynamics of state-feedback controller. The nonlinear backstepping controller depicted some initial oscillations, which died down once the controller settled to steady state value. Whereas, the nonlinear synergetic controller can be observed as initially slow to respond, yet it settled to its final dosage value of 3.22×10^5 $molecules\mu l^{-1}$ within 500 days.

*4.3. **P**erformance during Stage-2 HIV (using HIV dynamics given in eq.(1))*

The advancement of HIV infection from stage 1 to 2 is marked with a dwindling CD4 count, below the threshold of 500 $cells\ \mu l^{-1}$. The disease firmly establishes itself in stage-1 and the body is now weakened enough for opportunist diseases to attack. However, a sort of equilibrium is achieved after stage-1 and the virus particles don't multiply according to the same rate as in stage-1. Hence,

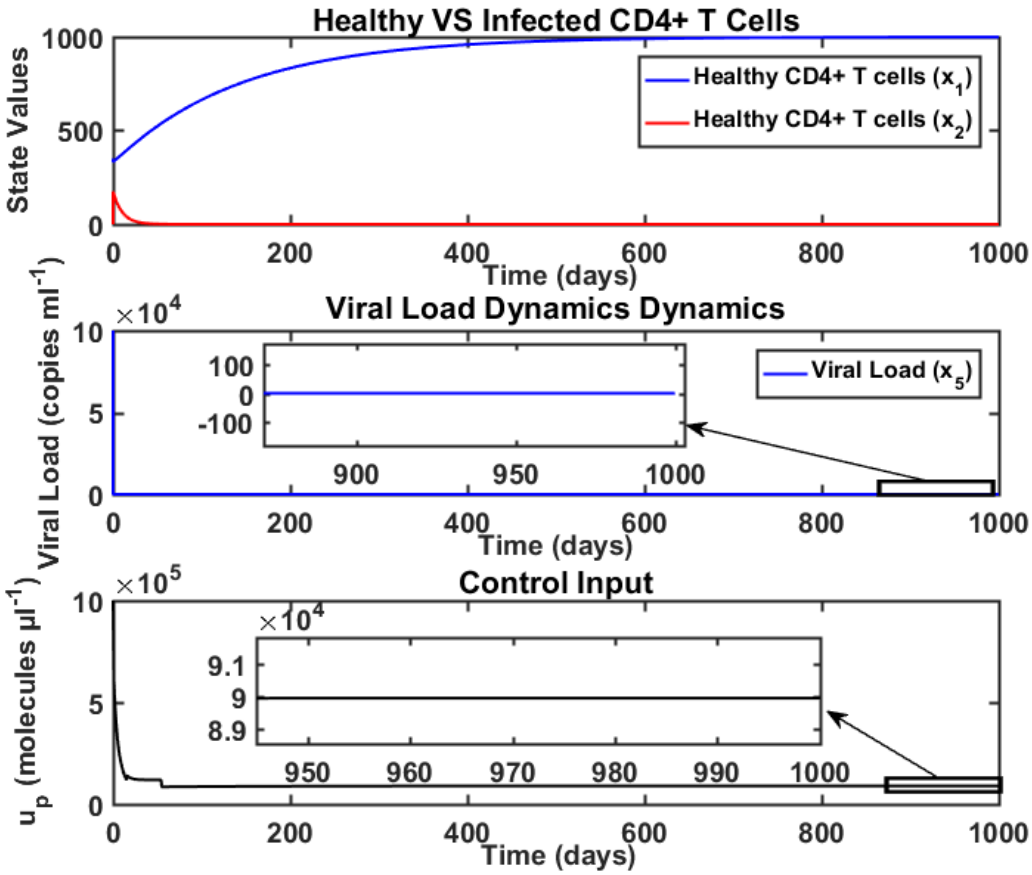


Figure 10: System Dynamics Stage-2 HIV- Proposed Sigmoid SMC-based MPC

the infection takes around a decade to progress further from stage-2 to stage-3 or AIDS when the CD4 count eventually drops below 200 $cells\ \mu l^{-1}$. Hence, to study the disease in stage-2, initial value of x_1 is set at 350 $cells\ \mu l^{-1}$ i.e. greater than 200 $cells\ \mu l^{-1}$ and less than 500 $cells\ mm^{-3}$. Similarly, the viral load of 100,000 $copies\ ml^{-1}$, considered to be high for HIV infection, is set as the initial value for stage-2 HIV dynamics.

Fig.(10) depicts the response of system dynamics under the impact of proposed algorithm for reduction of HIV viral load. The proposed controller once again reduced the viral load effectively. Similarly, the obtained state trajectories are also smooth and free of chattering. The dynamics of healthy CD4+ T cells once again reached steady state within 400 days. The initial drop in healthy cell population is negligible. The infected CD4+ T cells were also reduced to zero. Whereas, the

initial and final dosage administered by the proposed algorithm are 10×10^5 $molecules\mu l^{-1}$ and 9×10^4 $molecules\mu l^{-1}$ respectively. The detailed performance comparison between the proposed algorithm and the other recently proposed controllers is provided below:

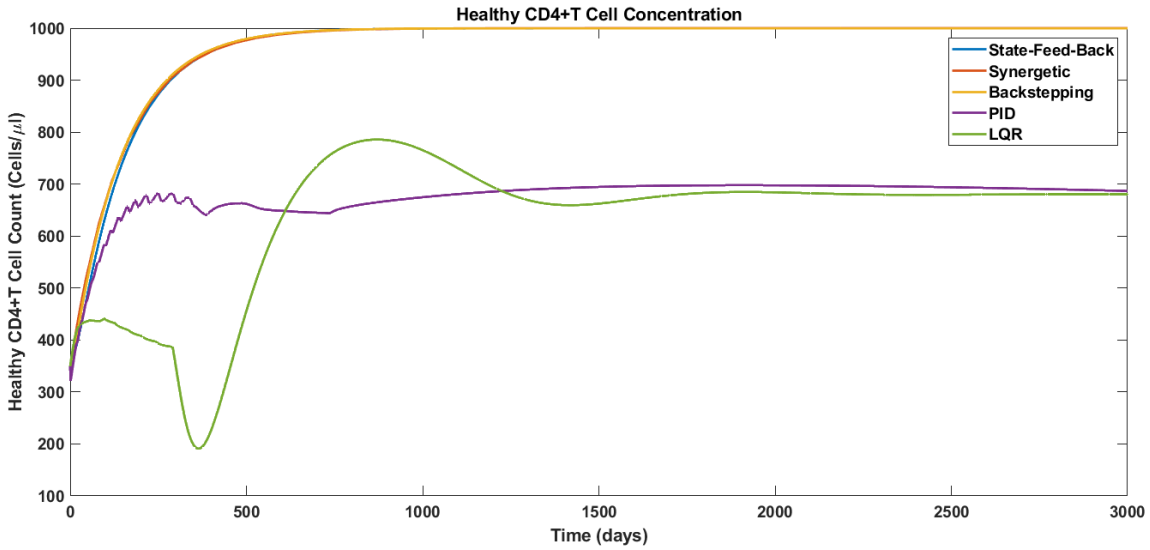


Figure 11: Healthy CD4+T Cell Concentration

4.3.1. Comparison of Healthy & Infected CD4+T Cells Dynamics

Fig.(11) depicts the response of healthy CD4+T cells undergoing anti-HIV therapy using different recently proposed feedback controllers. A similar response to that of the stage-1 curves is observed. The nonlinear controllers outperform the linear controllers again as they were the most expeditious. In case of backstepping controller, the steady state is reached in about is 557 days. The value is 565 days for state-feedback controller and 600 days for Synergetic controller. The linear PID controller did not depict any big undershoot or overshoot, though it still depicted a delayed response, especially in comparison to the non linear controllers. The LQR controller depicted the most delayed response and a big undershoot along with an overshoot can be observed. Lastly, a huge steady state error can be observed again, in the case of linear controllers, indicating their inability to contain the infection and the associated deterioration of the immunity and overall health.

Fig.(12) depicts the dynamics of the infected CD4+T cells. The linear controllers once again were

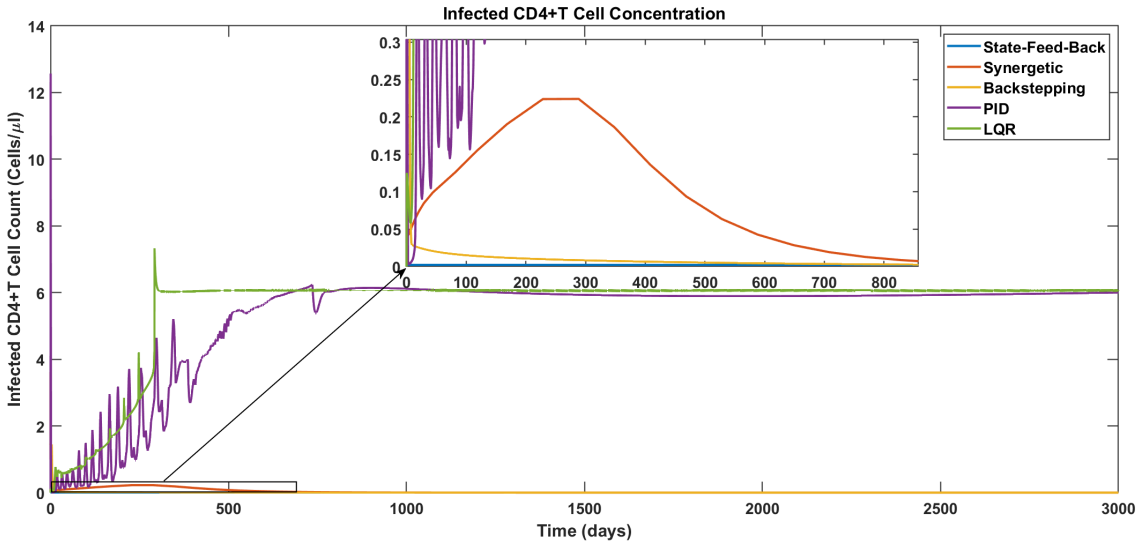


Figure 12: Infected CD4+T Cell Concentration

unable to completely eradicate the infected cells. However, the nonlinear controllers successfully converged the infected cells to 0. Since, the linear controllers were sluggish to act against the nonlinear nature of the system, hence, both the PID and LQR controllers resulted in a sustained population of infected cells, ensuring the survival and duplication of the virus copies in future. Among the nonlinear controller, allowed a small concentration of infected CD4+T cells.

*4.3.2. **V**iral Load Comparison*

The dynamics of the viral load has been depicted in fig.(13). Although all the nonlinear controllers were able to successfully reduce the viral load, yet only synergetic and backstepping controllers illustrated the convergence of viral load towards zero. The LQR controller was able to limit the increase in the viral load. But it was unable to converge it to 0, indicating a its sluggish response in determination and adjustment of drug dosage. Similarly, PID was the worst controller in terms of minimizing the viral load, as the load keeps on increasing over the span of the observed duration. The state-feedback controller was unable to diminish the viral load completely. Instead, after 3000 days, the state-feedback controller was able to bring the viral load to a low value of 3.5 $copies\ ml^{-1}$. In contrast, the proposed sigmoid SMC based MPC algorithm successfully reduced the viral load and converges it to zero. And this feat is achieved in least amount of time as well.

Lastly, the nonlinear synergetic controller depicted a small peak in Fig.(12), indicating an in-

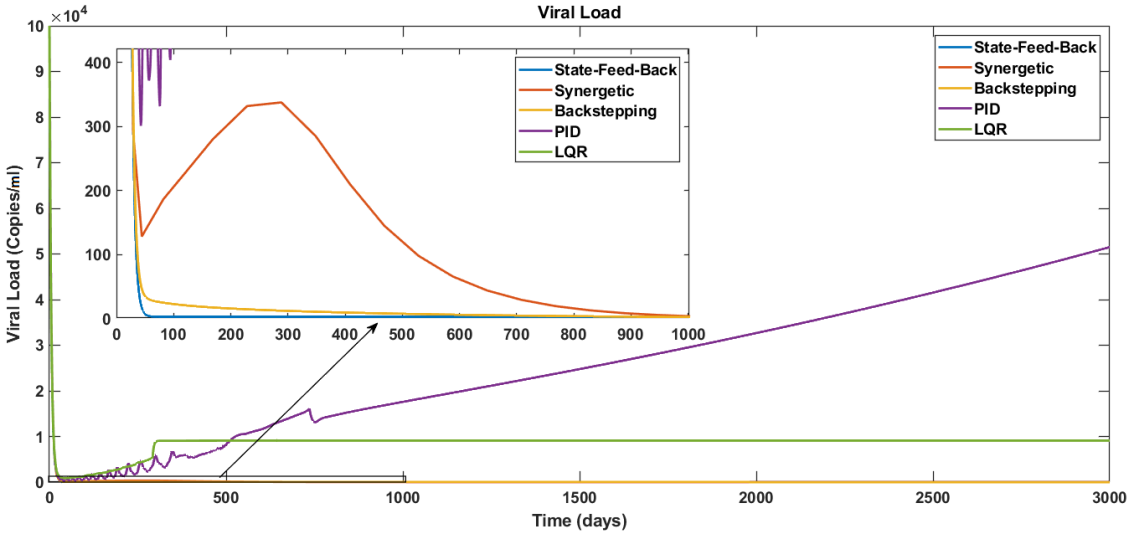


Figure 13: Total Viral Load

crease in infected cell population for a small span of time. This small peak results in the production of a small peak of viral load, as depicted in Fig.(13). As the infected cells results in the production of viral copies, hence, any increment in infected cell population results in an increment in the viral load as well.

*4.3.3. **D**rug Dosage Comparison*

For stage-2 HIV infection, the administered drug dosage by the designed controllers is shown in fig.(14). The LQR controller initiated the drug dosage with a very high peak of about $5 \times 10^5 molecules\mu l^{-1}$ but then falls to a very low value, and eventually stabilizes at around $1.4 \times 10^4 molecules\mu l^{-1}$. However, when the viral load dynamics, depicted in fig.(13) are studied side by side with the drug dosage, it can be inferred that the drug dosage must increase to curb the sustained values of viral load. Similarly, the response of PID controller was very slow as the controller kept increasing drug dosage even after 3000 days. As a result, the viral load had enough time to show substantial growth, and hence, the CD4 count also depicted substantial deterioration along with a receding trend, as shown in fig.(11).

Among the nonlinear controllers, the synergetic controller was also slow to react as drug dosage was very low and took some time to adjust itself. It reaches final steady state dosage of around $3.2 \times 10^5 molecules\mu l^{-1}$ in about 550 days. The backstepping controller started its feedback action

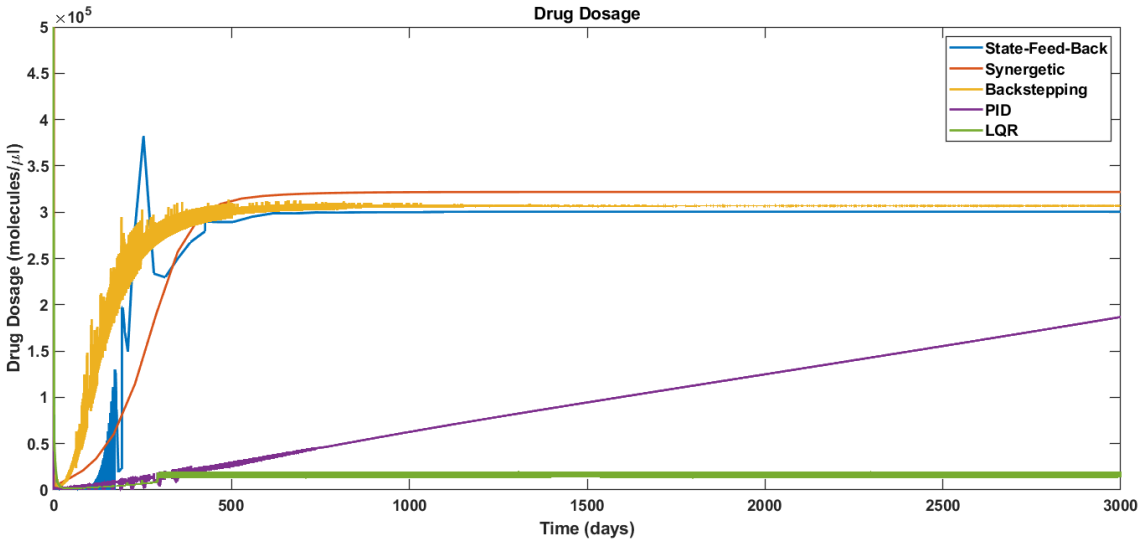


Figure 14: Control Input - Drug Dosage

from the initial dosage of $1.2 \times 10^5 molecules\mu l^{-1}$ and depicted a settling time of 450 days to achieve a final dosage of $3.06 \times 10^5 molecules\mu l^{-1}$. A similar response was observed for state-feedback controller and the initial dosage of $1.4 \times 10^5 molecules\mu l^{-1}$ was observed. However a peak response witha maximum value of $3.82 \times 10^5 molecules\mu l^{-1}$ was also observed. The response depicted a settling time of 395 days and the final drug dosage is settled at $3 \times 10^5 molecules\mu l^{-1}$. Although the nonlinear controllers outperformed linear algorithms, yet these controllers performed poorly in comparison with the proposed hybrid SMC-MPC algorithm. The proposed algorithm achieved steady drug dosage values in about 70 days. Similarly, the final dosage value of $9 \times 10^4 molecules\mu l^{-1}$ is also about 70% lower in comparison to the conventional nonlinear controllers.

*4.4. **P**erformance during Stage-1 HIV (using HIV dynamics given in eq.(2))*

For HIV dynamical model provided in eq.(2), identical initial conditions of the states for HIV-stage-1 have been utilized to verify the performance of proposed control algorithm. Moreover, as this model (eq.(2)) demands control of multiple inputs in combination, thus, the performance of proposed algorithm can be verified in this multi-input scenario as well. Commencement of cART at early stages can be proved to more potent against the HIV proliferation as the patients immunity is still intact and the harmful impacts of treatment therapy and the disease has not yet fatigued the body and its immune system's response. According to the model presented in eq.(2), the

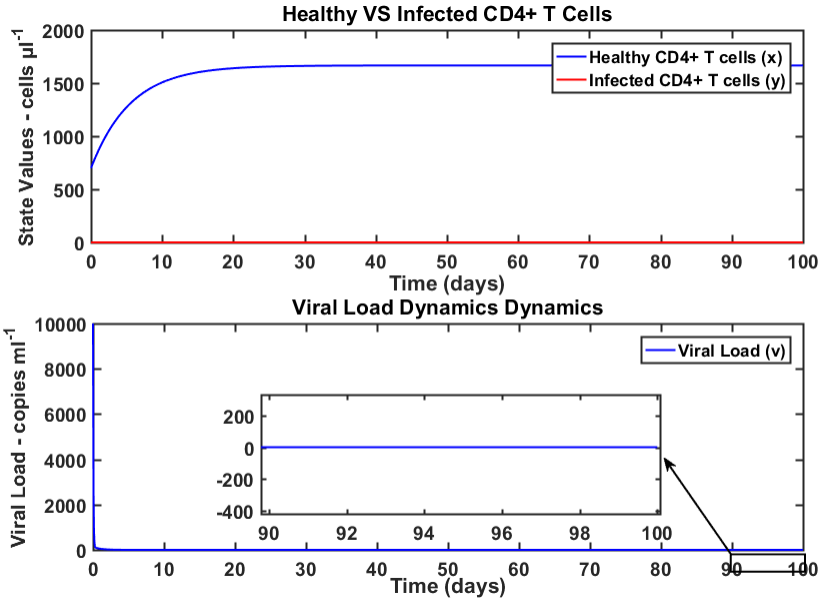


Figure 15: System Dynamics Stage-1 HIV- Proposed Sigmoid SMC-based MPC for Three Input Three State Model

maximum CD4 count for a healthy person can be found using steady state. This value hovers around 1666 $cells\ \mu l^{-1}$. The CD4 count for the affected person should not fall below 250 $cells\ \mu l^{-1}$, as the opportunistic diseases will kick in and the person won't be able to recover from that. If left untreated, the virus causes CD4 count to fall up to 500 $cells\ \mu l^{-1}$ during stage-1 HIV. Thus, to study the disease in stage-1, initial value of x is set at 700 $cells\ \mu l^{-1}$. Similarly, the viral load of 10,000 $copies\ ml^{-1}$, considered to be low for HIV is set as the initial condition for stage-1 HIV.

Fig.(15) depicts the response of system dynamics when proposed sigmoid SMC-based MPC algorithm is utilized for reduction of HIV viral load. These observed states have been under the coordinated action of three independently regulated control channels, depicted in Fig.(16). Once again, the proposed controller successfully reduced the viral load effectively and swiftly, while maintaining smooth and transient free state trajectories. In contrast to ART, the cART proved exceptionally more effective as the coordinated effort of the three independently regulated inputs boosts the CD4 count to reference levels within 15 days of therapy initiation. At each control update, the FI, RTI and PI inputs are computed in parallel, with their magnitudes determined according to the instantaneous system state and the adopted optimization objective. Similarly, the viral load has been reduced swiftly as well. However, as the HIV copies do not completely diminish

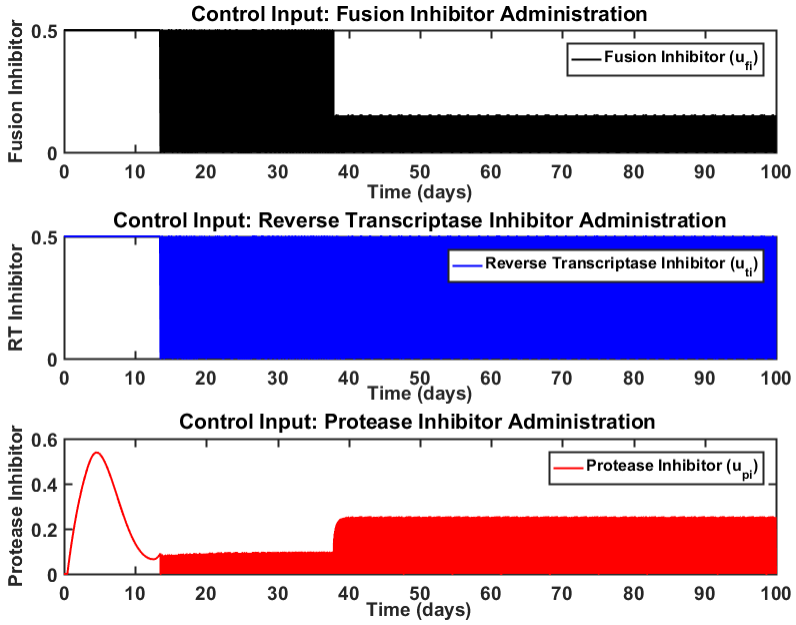


Figure 16: Administered Control Inputs by Proposed Sigmoid SMC-based MPC for Three Input Three State Model

from the body (evident from the inclusion of parameter λ_y, which keeps on producing virus copies), hence, the proposed algorithm keeps on administering the considered anti-viral cART drugs. This observation is consistent with the intended use of the model for representing persistent HIV-related dynamics. However, the present simulation should not be interpreted as establishing a clinical requirement for lifelong administration or as determining an appropriate treatment duration for patients. Thus, an algorithm capable of dynamically adjusting drug dosages in response to real-time disease progression is of critical importance. As the administration of excessive anti-viral drug dosages may lead to adverse side effects that outweigh therapeutic benefits, due to the inherent toxicity of these agents.

*4.5. **P**erformance during Stage-2 HIV (using HIV dynamics given in eq.(2))*

For stage-2 HIV using dynamical model provided in eq.(2), identical initial conditions of the system states have been utilized to verify the performance of proposed control algorithm. The advancement of infection from stage 1 to 2 results in the fall of CD4 count below 500 $cells\ \mu l^{-1}$, marking that the disease has progressed to an advanced stage. Once again, the aim of proposed algorithm is to improve the CD4 count, while allowing the viral load to be reduced on its own by

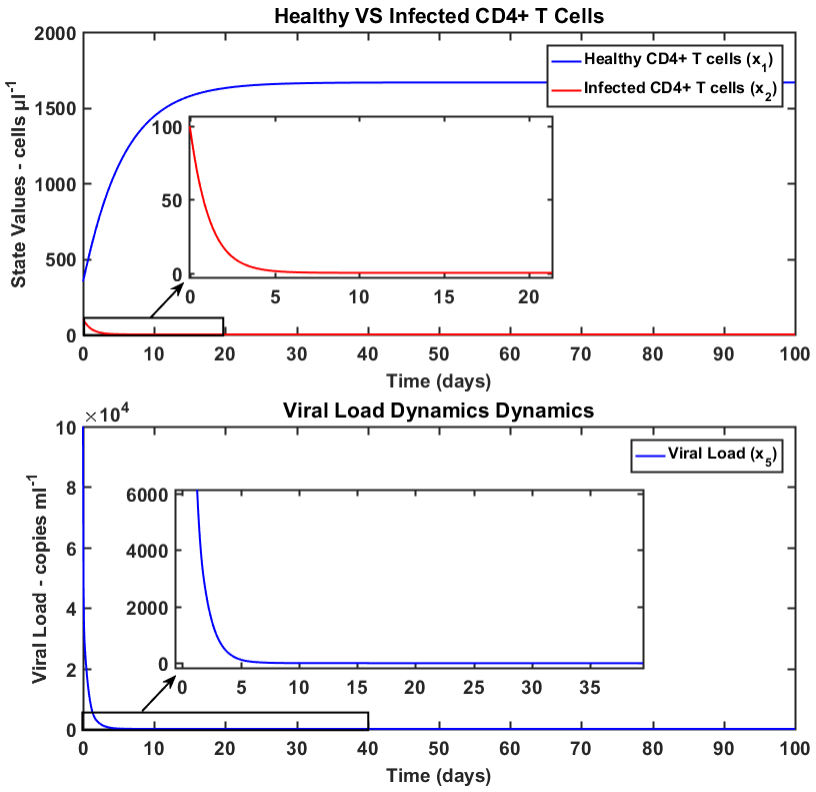


Figure 17: System Dynamics Stage-1 HIV- Proposed Sigmoid SMC-based MPC for Three Input Three State Model

the combined effort of FIs, RTIs, and PIs. Because, if the CD4 count falls below the level of 200 $cells\ \mu l^{-1}$, then the disease has officially progressed to stage-3. To imitate initial conditions of the system in stage-2, the initial value of state x is set at 350 $cells\ \mu l^{-1}$ i.e. greater than 200 $cells\ mm^{-3}$ and less than 500 $cells\ \mu l^{-1}$. Similarly, the viral load of 100,000 $copies\ ml^{-1}$, considered to be high for HIV infection, is set as the initial value for stage-2 HIV dynamics.

Fig.(17) depicts the response of system dynamics when proposed sigmoid SMC-based MPC algorithm is utilized for reduction of HIV viral load. The dynamics of states depicted in Fig.(17) have been observed under the combined impact of three independently regulated control inputs, depicted in Fig.(18). Once again, due to the effective management and administration of these drugs, the proposed controller successfully reduced the viral load effectively and swiftly, while maintaining smooth and transient free state trajectories. Similarly, in case of stage-2 HIV, cART enhanced by the proposed algorithm proved very potent as the combined impact of three independently regulated

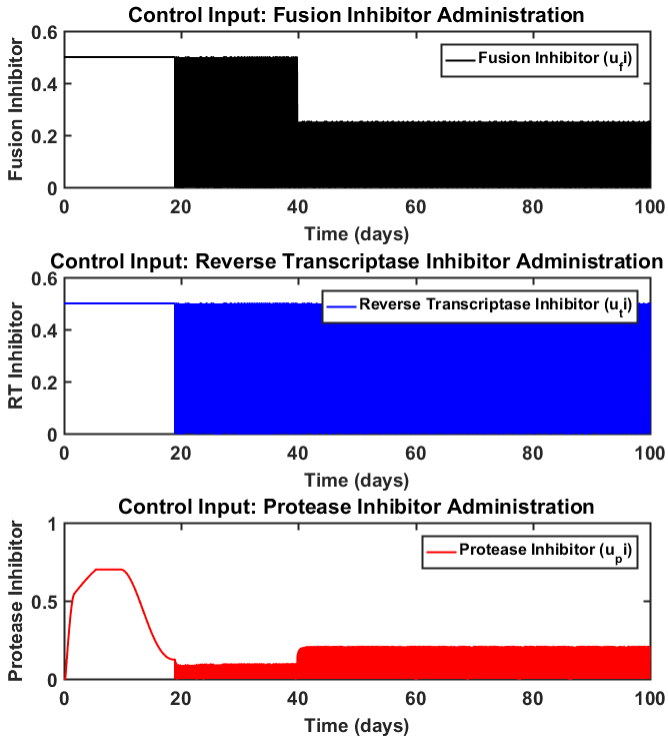


Figure 18: Administered Control Inputs by Proposed Sigmoid SMC-based MPC for Three Input Three State Model

inputs boosts the CD4 count to reference levels within first three weeks of therapy initiation.

Similarly, proposed control strategy worked well during stage-2 of disease progression as well. Once again, even though the algorithm efficiently reduced the viral load, yet due to the latently infected CD4+ T cells, an HIV affected person has to continue the cART medication to manage and contain HIV. Thus, owing to the chronic infection caused by HIV and the side-effects caused by the anti-retro-viral drugs, the impact of proposed approach to manage cART drug dosages based on the real-time indicators of disease progression has once again proved potent to contain HIV in stage-2.

It is important to note that the state trajectories shown in Fig.(15) and Fig.(17) results from the coordinated action of the three independently regulated control channels presented in Fig.(16) and Fig.(18) respectively. Because the proposed formulation permits the FI, RTI, and PI inputs to vary independently, their simulated profiles need not remain identical at every instant. This behavior reflects the mathematical flexibility of the multi-input controller rather than a proposed clinical

dosing schedule. The purpose of this simulation is to evaluate whether the nonlinear controller can regulate multiple drug-action pathways within the considered HIV dynamical model.

The control-input trajectories Fig.(16) and Fig.(18) should be interpreted in the context of parallel multi-input control formulation. At each control update, the proposed algorithm computes the FI, RTI, and PI inputs in parallel, while allowing their magnitudes to differ according to the instantaneous system state and the optimization objective. The fact that the three trajectories are not identical at every instant therefore does not imply that the corresponding treatments are administered sequentially or that the effect of one treatment is assumed to vanish before another becomes active. Rather, the trajectories describe controller's instantaneous regulation of three modeled drug-action pathways whose influence is incorporated into the subsequent evolution of the HIV states. This distinction is important because the present study evaluates the mathematical behavior of a multi-input nonlinear controller; it does not prescribe a time-separated clinical dosing schedule. Explicit pharmacokinetic/pharmacodynamic persistence and clinically constrained regimen design are beyond the scope of the present model and are identified as directions for future work.

4.6. ***Statistical Analysis***

To further validate the performance of the proposed sigmoid-SMC based MPC algorithm statistically, the simulations based experiment performed in subsections 4.2 and 4.3 were repeated 40 times with slightly modified initial conditions of healthy CD4+T cell count and Viral load, while keeping the remaining parameters and conditions unchanged. The obtained results were recorded. Independent T-tests are then performed to statistically validate the superiority, robustness and effectiveness of the proposed controller.

4.6.1. ***T-Test - Faster Viral Load Convergence Time Analysis***

Firstly, independent T-test is conducted to determine either proposed hybrid SMC and MPC based approach or the recently proposed conventional linear and nonlinear algorithms can swiftly converge HIV viral load to zero. Data from numerous recently proposed algorithms is utilized to perform this statistical analysis. The conventional algorithms proposed by [19, 27, 17, 30, 24] are re-implemented again to conduct this research study. Thus, to perform the experiment, two groups are considered, with each distinct values representing the time taken by the treatment procedure in days to completely converge Viral load to zero. The values of group1 depicts the time taken by the

proposed sigmoid SMC-based MPC algorithm to converge viral load to zero. Similarly, entries of group2 represent the time consumed by conventional backstepping, synergetic, state-feedback and optimal LQR controllers to converge HIV viral load to zero. The considered values of each groups are given below:

group1 = [32, 33, 33 ,34, 36, 37, 37, 36, 38, 31, 41, 37, 38, 39, 37, 42, 47, 43, 44, 48, 51, 55, 50, 52, 48, 37, 36, 38, 47, 51, 52, 50, 44, 45, 46, 47, 42, 43, 52, 37] (Sigmoid SMC-based MPC)

group2 = [64, 64, 67, 63, 72, 70, 75, 76, 299, 150, 300, 145, 253, 260, 309, 303, 2897, 2900, 2750, 2850, 2980, 2975, 1650, 1760, 1300, 2975, 2927, 1500, 1200, 2855, 2897] (Conventional Controllers)

Null Hypothesis: The following null hypothesis is considered while performing the independent T-test: *There is no significance difference between the mean time taken for the treatment between the two considered groups.*

Results: The obtained results after conducting the statistical analysis are given below:

1. Hypothesis Test Result (h) = 1 : thus, null hypothesis is rejected
2. p-value = $4.2794 \times 10^{-08} < 0.05$
3. tstat = -6.159 : which indicates that group1 or proposed sigmoid SMC-based MPC approach took significantly less mean time to suppress viral load.
4. Degree of freedom (df) = 69
5. Standard deviation (sd) = 824.73 : indicates that the data entries of considered groups, especially for group2, varies considerably.

Significance: After conducting the statistical analysis, the obtained results confirms and validates the hypothesis that the proposed sigmoid SMC-based MPC algorithm reduces the viral load more efficiently and swiftly in comparison to other conventional approaches.

4.6.2. ***T-Test - Faster CD4+ T Cell Count Augmentation Time Analysis***

The T-test is repeated to statistically compare the time taken by the considered algorithms for CD4 cell count improvement. The null hypothesis considered for this experiment is as follows:

Null Hypothesis: *There is no significance difference between the mean time taken for CD4 count improvement between the two considered groups.*

The following two groups are considered:

group1 = [255, 257, 257 ,258, 260, 262, 263, 259, 266, 251, 285, 264, 266, 266, 267, 290, 307, 287,

300, 297, 305, 368, 350, 355, 292, 267, 259, 263, 296, 319, 323, 315, 295, 297, 293, 299, 288, 285, 235, 261] (Proposed Sigmoid SMC-based MPC)
group2 = [380, 385, 410, 372, 490, 467, 503, 515, 1176, 702, 1233, 656, 878, 937, 1500, 1275, 566, 575, 550, 570, 580, 593, 515, 523, 517, 597, 575, 520, 500, 551, 565] (Recently proposed conventional algorithms)

Results:

1. Hypothesis Test Result (h) = 1 : thus, null hypothesis is rejected
2. p-value = $10497 \times 10^{-11} < 0.05$
3. tstat = -81529 : which indicates that group1 proposed algorithm took significantly less mean time to improve healthy CD4+ T cell count.
4. Degree of freedom (df) = 69
5. Standard deviation (sd) = 187.75 : indicates that the entries of considered data varies considerably.

Significance: The provided results of the statistical analysis emphasis that the mean time taken by group1 or proposed sigmoid SMC-based MPC algorithm is significantly different than the mean time taken by conventional algorithms to improve and maintain a healthy CD4 count.

5. Discussion: Comparison between Analyzed Techniques

The observations and results, presented in Section 4 have been comprehensively presented in tabular form in tables tab.(4), tab.(5), tab.(6) and tab.(7). Tab.(4) compares the performance of the controllers while improving the healthy CD4+T cell count. Whereas, tab.(5) analyzes and compares the performance of the controllers in curbing viral load. Similarly, tab.(6) analyzes the drug dosage (and its dynamics) administered by each controller to execute ART. Lastly, tab.(7) analyzes and compares the performance of recently presented multi-input optimization based algorithm with the proposed sigmoid SMC based smooth MPC algorithm for the execution of cART. The comparative analysis of the controller's performances in tab.(4), is established based on Rise Time (RT), Settling Time (ST; 2% and 5 % criteria), Steady State Error (SSE), Overshoot and Undershoot. The Rise time is considered to be the shortest time taken by the dynamics to reach 90% of its final value. Similarly, settling time is decided based on two criteria, i.e. the time taken by the dynamics or

curve to reach with in the 5% and 2% limit of the final or steady state value. The steady state error is considered to develop a comparison with the ideal or healthy conditions of a human body. Lastly, in order to further validate the performance of proposed algorithm, its ability to implement cART is analyzed and compared with recently presented algorithms in tab.(7). This comparison is established on the basis of six different metrics. These criterion analyzes the capability of considered algorithms to converge viral load, infected CD4+ T cells and healthy CD4+ T cells to their desired steady state values. Similarly, the table also informs whether the considered control technique results in any harmful drop in CD4 count or not. Lastly, the drug dosage dynamics are also considered along with settling time for the three states x (healthy CD4+ T cells), y (infected CD4+ T cells) and v (mature infectious virus particles), to establish a sound comparison.

Table 4: Controller Performance Comparison - Healthy CD4+T Cells Dynamics

Method	Parameter	RT (days)	ST 2% (days)	ST 5% (days)	Overshoot ($cell\ \mu l^{-1}$)	Undershoot ($cell\ \mu l^{-1}$)	SSE ($cell\ \mu l^{-1}$)
PID	x_1 stage-1	1165	1888	1479	NIL	200	165
	x_1 stage-2	130	985	772	NIL	28	312.7
LQR	x_1 stage-1	315	649	511	NIL	410	111
	x_1 stage-2	586	1550	1145	105	160	319.5
Synergetic	x_1 stage-1	164	512	362	NIL	NIL	0
	x_1 stage-2	280	527	490	NIL	2	0
State-Feedback	x_1 stage-1	170	501	377	NIL	NIL	0
	x_1 stage-2	285	515	482	NIL	NIL	0
Backstepping	x_1 stage-1	207	550	410	NIL	NIL	0
	x_1 stage-2	272	502	473	NIL	1.5	0
Proposed	x_1 stage-1	168	380	265	NIL	35	0
Algorithm	x_1 stage-2	266	488	368	NIL	2	0

By analyzing the data presented in tab.(4), it can be observed that the linear controllers not only depicted sluggish responses in improving the CD4 count in both the stages, but they also depicted undershoots and steady state errors. The existence of undershoot alone is very alarming as any steep drop in CD4+T cells brings in the possibility for the opportunistic diseases to attack

the weakened human body. Similarly, the nonlinear controllers performed very similar to each other. However, based on rise time and settling time comparison, the proposed nonlinear sigmoid SMC-based MPC algorithm outperforms the remaining two.

The best possible condition for an infected person is to have a viral load as low as possible, i.e. ideally it should be zero. Similarly, the healthy CD4+T count should be as close to the average CD4 count of a healthy person, as possible, i.e. about 1000 $cell\ \mu l^{-1}$ (although this amount varies from person to person, yet a CD4 count of 1000 $cell\ \mu l^{-1}$, especially in HIV positive patients is considered exceptionally good). Hence, table.(5) compares the performance of the designed controllers for the problem of viral load reduction, based on settling time, overshoot, steady state error, the ability of the controller to converge the viral load to zero and lastly, the trend of the viral growth. The performance of the synergetic, state-feedback and backstepping controller is represented as Syn, S-FB and BS, respectively under the method column in tab.(5).

The linear PID controller depicted an ever increasing viral growth (represented as EI in tab.(5)) and hence, the settling time is unable to measure, as the dynamics didn't settle down throughout the simulated duration. Hence, the viral dynamics depicted huge steady state errors and thus, it using PID controller for the application of ART seems very perilous. The CIT under the column of Viral growth in tab.(5) represents continuously increasing trend. The LQR controller depicted somewhat better response in comparison to that of PID, as the controller act swiftly to adjust the dosage to reduce viral load, however, once the viral load was reduced, the controller was unable to maintain a continuously reducing trend of viral load, instead, the viral load start increasing steadily and eventually, some sort of equilibrium seems to be achieved,a s the viral load becomes constant. However, the viral load in both stage 1 and 2 of HIV remained lower than 10,000 $copies\ ml^{-1}$, hence, the LQR controller does succeed to lower down the viral load. Thus the viral growth trend has been categorized as SLL (Stable at relatively low viral load).

The nonlinear controllers once again depicted exceptional performance characteristics as reduced the viral load to extra ordinary low levels. In fact a viral load of less than 50 $copies\ ml^{-1}$ is extremely difficult to detect using current testing mechanisms. All the nonlinear controllers manifested a downward trend of reducing viral load, signifying their ability to continuously reduce any produced virus copies. However, the settling times of synergetic and backstepping controllers are suggesting a sluggish response. Similarly, the state-feedback controller tends to maintain a very low amount of viral load and is unable to converge it towards zero. Thus, for state-feedback controller, the viral

Table 5: Controller Performance Comparison - Viral Load Dynamics

Method	Parameter	ST 2% (days)	ST 5% (days)	Overshoot ($copies/ml$)	SSE ($copies/ml$)	Convergence Yes\No	Viral Growth
PID	VL stage-1	—	—	EI	1×10^3	No	CIT
	VL stage-2	—	—	EI	5.05×10^4	No	CIT
LQR	VL stage-1	253	145	5.7	1157	No	SLL
	VL stage-2	303	299	9210	9100	No	SLL
Syn	VL stage-1	2980	2900	111	0.0	Yes	CRT
	VL stage-2	2975	2897	337	0.0	Yes	CRT
S-FB	VL stage-1	70	64	NIL	0.653	No	SVLL
	VL stage-2	72	64	NIL	3.28	No	SVLL
BS	VL stage-1	1650	1300	NIL	0.078	Yes	CRT
	VL stage-2	2975	2927	NIL	0.74	Yes	CRT
Proposed Algorithm	VL stage-1	49	38	NIL	0.00	Yes	CRT
	VL stage-2	61	55	NIL	0.00	Yes	CRT

growth is categorized as: SVLL, i.e. stable at very low viral load.

Whereas, the synergetic and backstepping controllers manifested an exponentially reducing viral growth trend. The Viral growth trend for synergetic and backstepping controller is hence categorized as CRT, i.e. continuously reducing trend. On the other hand, the proposed sigmoid SMC-based MPC algorithm depicted extremely fast convergence rate, along with zero steady state error and continuously reducing trend (mentioned as CRT in tab.(5)) for viral growth

Lastly, tab.(6) compares the dynamics of the administered drug dosage by each designed and considered controller. The drug dosage should be with in the well defined limits as an over dosage of protease inhibitor is equivalent to the injection of life threatening toxins in a human body. Hence, this performance comparison among the controllers is established, based on initial and final dosage, settling time and dosage trend. The PID controller exhibited a continuously increasing trend (mentioned as CIT in tab.(6)) of drug dosage and hence the dosage never settled to a steady state value for PID controller in both stage 1 and 2 of HIV infection. On the other hand, the LQR controller depicted high initial dosage but comparatively low final dosages. Moreover, the dosage

Table 6: Controller Performance Comparison - Drug Dosage Dynamics

Method	Parameter	Initial Dosage ($mol\ \mu l^{-1}$)	Final Dosage ($mol\ \mu l^{-1}$)	ST 2% (days)	ST 5% (days)	Dosage Trend
PID	u stage-1	6.8×10^6	1.3×10^5	—	—	CIT
	u stage-2	6.3×10^6	1.85×10^5	—	—	CIT*
LQR	u stage-1	2×10^7	2000	—	—	Stable
	u stage-2	2×10^8	1.7×10^4	—	—	Stable
Synergetic	u stage-1	1.355×10^6	3.22×10^5	470	400	Stable
	u stage-2	1.3×10^6	3.2×10^5	558	430	Stable
State-Feedback	u stage-1	1.6×10^9	3×10^5	440	320	Stable
	u stage-2	1.6×10^9	3×10^5	560	430	Stable
Backstepping	u stage-1	2.2×10^6	3.05×10^5	2424	2139	Stable
	u stage-2	2.4×10^6	3.06×10^5	650	454	Stable
Proposed	u stage-1	9.9×10^5	8.78×10^4	89	43	Stable
Algorithm	u stage-2	10×10^5	9×10^4	186	88	Stable

dynamics depicted sufficiently large oscillations. Thus, for PID and LQR controllers, the 2% or 5% criteria for settling time is never met. However, if 15% criteria is considered, i.e. the duration required by the dynamics to reach within 15% of the final or steady state value, then the LQR controller took around 450 and 500 days to settle.

Among the nonlinear controllers, the state-feedback controller depicted very high initial dosage, and eventually settled at the final dosage of 3×10^5 ($molecules\ \mu l^{-1}$). Moreover, another important observation is the manifestation of oscillations in the response using backstepping controller, resulting in a large settling time. Similarly, the synergetic controller depicted moderate initial and final dosages of 1.3×10^6 ($molecules\ \mu l^{-1}$), and 3.2×10^5 ($molecules\ \mu l^{-1}$) respectively. The proposed sigmoid SMC-based MPC algorithm settled to its steady state values very swiftly and did not depict any notable oscillation as well. Moreover, it also depicted the least initial and final dosages, making it the most efficient of the considered controllers.

As discussed in Section 1, the bulk of the recent research studies related to the drug regulation of anti-HIV drugs for ART, not only proposed linear controllers for the therapy, but they also

considered inadequate mathematical models as well. Similarly, the values of the parameters utilized in these models are also far from the actual real world scenarios. For instance, [19] considered a viral load of about 80 mg per liter, whereas, the standard units to measure viral load are expressed in copies per ml or copies per μl. Similarly, [21, 20] utilized fictitious initial conditions of state variables as well. However, this study considered realistic values of high and low viral load, i.e. if the viral load is less than 10^4 $copies\ ml^{-1}$, it is considered low and if it is greater than 10^5 $copies\ ml^{-1}$, the the viral load is considered high [45, 46].

To prove the adaptability and flexibility of the proposed sigmoid SMC based smooth MPC algorithm for anti-HIV therapy, its performance is compared with the recently presented techniques in literature. The proposed multi-input algorithm, designed in subsection 3.5.2 based on model presented in eq.(2), utilized FI, RTI and PI in combination to effectively curb infection and devastation caused by HIV. The performance comparison between the proposed multi-input smooth SMC based MPC algorithm and recently presented control techniques is provided in tab.(7). The first parameter of comparison is the ability of the considered control techniques to converge the viral load towards undetectable levels. Only the algorithm proposed in Ref. [22] failed to substantially lower the viral load, which explains the numerous falls in healthy CD4+ T cell dynamics, that are definitely highly unwanted and may result in severe consequences for the patient under consideration. Similarly, the algorithm proposed in this study along with the one presented in ref.[28] are the only techniques that focused on decimation of infected CD4+ T cells. Improved CD4 count is one of the primary goal of any anti-HIV therapy. By analyzing tab.(7), it can be observed that the proposed sigmoid SMC based MPC algorithm very swiftly increase the CD4 count, as it is evident by observing the settling times of all three considered states as well. Lastly, the algorithms presented in Ref.([28, 25]) ended up converging the administered anti-HIV drugs to 0. As discussed earlier in section 4, the cART is a lifelong procedure against HIV proliferation as it is currently impossible to completely get rid of the disease itself. Thus by converging the control inputs to 0, these control techniques can create severe consequences for the patient under consideration as the HIV particles can replicate themselves at tremendously quick rates in the absence of anti-HIV drugs. Thus, even in managing multi-input cART procedure against HIV, the proposed smooth SMC based MPC algorithm outperformed other control techniques and proved to be highly flexible under varying initial conditions. Similarly, the proposed algorithm can accommodate different classes of drugs smoothly to match the requirements of the patient under consideration.

Table 7: Controller Performance Comparison - Multi-Input System

Reference	Viral Load Convergence	Convergence of y to 0	Increment in x	Max Fall in x	Dosage Trend	ST 2% (days)		
						x	y	v
[47]	Yes	No	Very Slow	10%	Stable	9000	5000	5000
[28]	Yes	Yes	Slow	NIL	converged to 0	>300	120	30
[25]	Yes	Moderate	Slow	NIL	converged to 0	200	30	50
[22]	No	No	Very Slow	80%	N\A	>700	N\A	>500
Proposed	Yes	Yes	Fast	NIL	Stable	45	10	15

As discussed in Section 1 and Section 5, this study emphasized on establishment and utilization of limits for treatment dosages so that an appropriate response that focuses on reduction in treatment burden may be realized. However, all of the recent research studies simply failed to establish such relationship between the control inputs and their limits. Similarly, this study has also proposed the need to avoid over dosage of the anti HIV drugs, as they are toxins, and are considered harmful for a healthy being. Lastly, this research work has proposed optimization based nonlinear control algorithm for drug regulation against HIV infection in simulation environment. This study is not guaranteeing the success of anti retro viral therapy against the HIV infection. The success of anti-viral therapy is directly dependent on the condition of patient's health, the situation of disease progression, the type of drug(s) and whether it is accepted by the patients' body or not, and numerous other physical, physiological and chemical factors. This study is also not suggesting any particular protease inhibitor or any other class of anti-retro-viral drug to any HIV infected patient, instead, this study utilized one of the common protease inhibitor used all across the globe to perform mathematical calculations so that a relationship may be established between the control input(s) and the drug dosage(s) currently administered by the physicians for anti-viral therapy against HIV.

6. Model Limitations and Drug-Resistance Considerations

An important limitation of the present multi-input formulation concerns the representation of combination anti-retro-viral therapy (cART). In the three-state model, the FI, RTI, and PI are represented as independent control inputs. The proposed controller computes these three treat-

ment inputs in parallel at each control update, while their magnitudes may differ according to the instantaneous system state and the adopted control objective. The resulting differences in the input trajectories, therefore, should not be interpreted as sequential administration in which one drug is necessarily withdrawn before another is applied. Rather, they represent the controller's instantaneous regulation of distinct drug-action pathways within the mathematical model. Moreover, the influence of the control inputs is propagated through the subsequent system dynamics and is not assumed to disappear instantaneously at the next control update. Nevertheless, because explicit pharmacokinetic and pharmacodynamic states are not included, the model does not quantify drug absorption, clearance, concentration persistence, or drug-specific exposure. Thus, this interpretation is limited to the dynamical representation adopted in the present study and should not be considered a clinical dosing prescription.

This distinction is particularly relevant when considering antiviral resistance. The present model does not explicitly represent viral genetic variation, mutation, drug-resistant sub-populations, or the evolutionary dynamics associated with different treatment exposures. Consequently, the present controller cannot evaluate whether a particular temporal pattern of the three inputs would increase or decrease the probability of resistance emergence. Previous studies have demonstrated the importance of combination therapy and the evolutionary consequences of antiviral treatment in determining resistance development [48, 49, 50]. The present work therefore does not claim that the independently optimized control trajectories constitute an optimal resistance-prevention strategy. Instead, the three-input simulation is intended to assess the algorithmic capability of the proposed nonlinear controller to regulate a multi-input HIV dynamical model. Incorporating resistance-aware viral dynamics together with pharmacokinetic/pharmacodynamic effects and clinically constrained cART regimens represents an important direction for future research.

7. Model Interpretation and Potential Implications

The results presented in this study should be interpreted primarily as a simulation-based evaluation of a nonlinear control framework rather than as evidence for clinical efficacy or a proposed treatment protocol. The mathematical models provide a controlled environment in which the proposed sigmoid SMC-MPC strategy can be compared with alternative controllers with respect to viral-load suppression, CD4+ T-cell recovery, and control-input regulation. The obtained results demonstrate the behavior of the proposed algorithm under the assumptions and parameter values

of the adopted models; they do not establish clinical safety, therapeutic efficacy, or suitability for direct administration to patients.

Several biological and treatment-related factors are not represented in the present formulation. In particular, the models do not explicitly describe viral genetic variation, the emergence and selection of drug-resistant viral strains, pharmacokinetic and pharmacodynamic effects, adherence, drug-drug interactions, intra-cellular drug concentrations, or patient-specific treatment constraints. The three-input model additionally treats FI, RTI, and PI as independently adjustable control variables. Therefore, the control trajectories should not be interpreted as recommended individual-drug schedules. A clinically meaningful control framework would require these constraints to be incorporated together with validated patient-specific models and established cART regimens. These extensions are reserved for future research.

The proposed smooth SMC based MPC algorithm is formulated with in a continuous-time framework that can incorporate a number of practical constraints and treatment objectives. The proposed optimal controller is designed to illustrate its potential for precise and flexible operation to contain HIV spread by managing viral load and immune response. Even though the proposed system assumes continuous dosage modulation, the algorithm can be easily discretized to accommodate fixed-dosage constraints. Similar concerns were raised in recent times for treatment of diabetes using automatic feedback-based insulin delivery systems. Previously, crude and fixed-dosage injections were administered to regulate blood-glucose level. Such practices often lead to hypoglycemia or poor blood glucose regulation in blood stream. However, with advancements in the field of biomedical engineering, smart insulin pumps and patches were developed based on feedback based systems to dynamically regulate blood glucose level through insulin administration.

Since, drug employed in cART against HIV are toxic in nature, thus over-dosage of these agents can cause severe harm to the affected patients. By employing feedback-based dynamical drug regulation system, such dosage related complications can be significantly managed. The proposed framework may be viewed as a preliminary computational step toward the study of feedback-based treatment-input regulation in biomedical dynamical systems. The continuous-time formulation also provides a basis for investigating constrained treatment-input optimization in future studies. However, translation of the proposed approach to an automated drug-delivery platform would require validated pharmacokinetic and pharmacodynamic models, clinically established treatment regimens, safety constraints, patient-specific physiological information, and extensive experimental

and clinical validation. Such implementation considerations are beyond the scope of the present simulation study.

8. Conclusion

This paper proposed nonlinear sigmoid SMC-based MPC algorithm for the managing anti-retro-viral therapy against the spread of HIV infection. The study also presented deterministic HIV - human immune system model and the design of proposed controller is based on it. The stability analysis of the system, based on Lyapunov stability theory has also been presented. To analyze the performance of designed controllers, MATLAB/Simulink has been utilized to perform simulations and observations, and results have been presented and discussed in great detail. To validate the performance of designed controller, extensive comparison with recently proposed linear and non-linear controllers such as State-feedback, synergetic, backstepping, PID and LQR have also been established. The merits and demerits of each controller have been discussed diligently. Overall, the simulation results indicate that the proposed sigmoid SMC-based MPC framework provides effective nonlinear regulation of the considered HIV dynamical models and achieves favorable performance in terms of viral-load suppression, CD4+ T-cell recovery, and control-input regulation under the adopted simulation conditions. The three-input study further demonstrates the flexibility of the proposed framework for systems containing multiple drug-action pathways. However, the present results are limited to deterministic mathematical models and should not be interpreted as evidence of clinical efficacy or as a recommendation for automated anti-retro-viral drug administration. In particular, the multi-input model treats the three drug classes as independently adjustable control channels and does not incorporate viral mutation, drug-resistant sub-populations, pharmacokinetics, pharmacodynamics, adherence, or drug-drug interactions. Future work will therefore focus on resistance-aware HIV models and clinically constrained cART formulations in which regimen composition, synchronized administration, and treatment-related biological constraints are explicitly incorporated into the control optimization problem.

Conflicts of Interest:

The authors declare no conflict of interest.

Ethical Approval:

The authors declare that no ethical approval is required for the publication of this study.

Credit authorship contribution statement:

Muhammad Arsalan: Conceptualization, Methodology, Software, Validation, Formal analysis, Investigation, Writing - original draft. **Sadiq Muhammad Tariq:** Validation, Formal analysis, Investigation, Writing - review & editing, Visualization, Supervision, Resource management. **Abubakar Rafique:** Writing - review & editing, Visualization. **Xiaojun Yu:** Writing - review & editing, Visualization, Supervision, Resource management.

References

[1] The National Institutes of Health, Lymphocyte (2023).
URL https://www.genome.gov/genetics-glossary/Lymphocyte

[2] K. Vidiya, K. P. Karthigeyan, S. P. Tripathi, L. E. Hanna, Pathphysiology of cd4+t-cell depletion in hiv-1 and hiv-2 infections, Frontiers in Immunology 8.

[3] S. Ray, U. Maulik, Discovering perturbation of modular structure in hiv progression by integrating multiple data sources through non-negative matrix factorization, IEEE/ACM Transactions on Computational Biology and Bioinformatics 15 (2018) 869–877. doi:10.1109/TCBB.2016.2642184.

[4] World Health Organization, HIV and AIDS (2023).
URL https://www.who.int/news-room/fact-sheets/detail/hiv-aids

[5] M. Ahsan, M. Saeed, A. Mehmood, The study of hiv diagnosis using complex fuzzy hypersoft mapping and proposing appropriate treatment, IEEE Access 8 (2021) 104405–104417. doi:10.1109/ACCESS.2021.3099335.

[6] The National Institutes of Health, Symptoms of HIV (2022).
URL https://www.hiv.gov/hiv-basics/overview/about-hiv-and-aids/symptoms-of-hiv/

[7] The National Institutes of Health, The Stages of HIV Infection (2021).
URL https://hivinfo.nih.gov/understanding-hiv/fact-sheets/stages-hiv-infection

[8] The National Institutes of Health, HIV Testing (2021).
URL https://hivinfo.nih.gov/understanding-hiv/fact-sheets/hiv-testing

[9] World Health Organization, HIV (2022).
URL https://www.who.int/health-topics/hiv-aids#tab=tab_1

[10] Centers for Disease Control and Prevention, Types of HIV Tests (2022).
URL https://www.cdc.gov/hiv/basics/hiv-testing/test-types.html

[11] P. D. Giamberardino, L. Compagnucci, C. D. Giorgi, D. Iacoviello, Modeling the effects of prevention and early diagnosis on hiv/aids infection diffusion, IEEE Transactions on Systems, Man, and Cybernetics: Systems 49 (2019) 2119–2130. doi:10.1109/TSMC.2017.2749138.

[12] K. D. Bui, C. A. Wamsley, F. S. Shofer, D. L. Kolson, M. J. Johnson, Robot-based assessment of hiv-related motor and cognitive impairment for neurorehabilitation, IEEE Transactions on Neural Systems and Rehabilitation Engineering 29 (2021) 576–586. doi:10.1109/TNSRE.2021.3056908.

[13] J. Shaw, N. Matin, Opportunistic infections in hiv, Medicine 50 (2021) 294–297. doi:https://doi.org/10.1016/j.mpmed.2022.02.010.

[14] IhsanUllah, S. Ahmed, Q. Al-Mdallal, K. Zareen, K. Hasib, K. Aziz, Stability analysis of a dynamical model of tuberculosis with incomplete treatment, Advances in Continuous and Discrete Modelsdoi:https://doi.org/10.1186/s13662-020-02950-0.

[15] L. Hu, P. Hu, X. Luo, X. Yuan, Z.-H. You, Incorporating the coevolving information of substrates in predicting hiv-1 protease cleavage sites, IEEE/ACM Transactions on Computational Biology and Bioinformatics 17 (2020) 2017–2028. doi:10.1109/TCBB.2019.2914208.

[16] A. M. N. Tsibris, M. S. Hirsch, Mandell, Douglas, and Bennett's Principles and Practice of Infectious Diseases (Eighth Edition), Vol. 1, 2015. doi:10.1016/B978-1-4557-4801-3.00130-2.

[17] R. Banerjee, R. K. Biswas, Mathematical model of hiv: A fractional optimal control based approach, in: International Conference on Communication, Control and Information Sciences (ICCISc), IEEE, 2021. doi:10.1109/ICCISc52257.2021.9484981.

[18] M. Khater, A. A.El-Syed, M. El-Shorbagy, Abundant stable computational solutions of atanganabaleanu fractional nonlinear hiv-1 infection of cd4+ t-cells of immunodeficiency syndrome, Results in Physics 22. doi:10.1016/j.rinp.2021.103890.

[19] R. Saeed, Butt, A. Iftikhar, I. Ramsha, M. Arsalan, Integral backstepping and synergetic control for tracking of infected cells during early antiretroviral therapy, IEEE Access 7 (2019) 69447–69455. doi:10.1109/ACCESS.2019.2907201.

[20] W.-J. Wang, Y. Ding, Hiv infection control design with the form of constant or state function, IEEE Access 7 (2019) 84282–84292. doi:10.1109/ACCESS.2019.2924459.

[21] C. Siriwan, R. Thienchai, W. Yukunthorn, Control theory for hiv dynamics: Sliding mode control in antiviral drug therapy, Journal of Physics: Conference Series 1. doi:10.1088/1742-6596/1144/1/012070.

[22] A. Landi, et al, Modelling and control of hiv dynamics, Results in Physics 89 (2008) 162–168. doi:https://doi.org/10.1016/j.cmpb.2007.08.003.

[23] M. Ghani, Dynamics of spatio-temporal hivaids model with the treatments of haart and immunotherapy, International Journal of Dynamics and Controldoi:https://doi.org/10.1007/s40435-023-01284-5.

[24] N. Ahmed, et al, Stability analysis and numerical simulations of spatiotemporal hiv cd4+ t cell model with drug therapy, Chaosdoi:10.1063/5.0010541.

[25] F. A. Edilson, et al, An optimal control approach to hiv immunology, Applied Mathematics 6 (2015) 1115–1130. doi:10.4236/am.2015.66102.

[26] H. Chang, A mathematical study on the drug resistant virus emergence with hiv/aids treatment cases, Heliyon 7. doi:https://doi.org/10.1016/j.heliyon.2020.e05883.

[27] S. Alsahafi, S. Woodcock, Exploring hiv dynamics and an optimal control strategy, Mathematics 10(5). doi:https://doi.org/10.3390/math10050749.

[28] P. Ngina, et al, Modelling optimal control of in-host hiv dynamics using different control strategies, Computational and Mathematical Methods in Medicine 2018. doi:10.1155/2018/9385080.

[29] Y. Liu, Feedback linearization and optimal design for the control of an hiv pathogenesis model, in: The 27th Chinese Control and Decision Conference, IEEE, 2015.

[30] Arsit B. and et al, Synergetic control for hiv infection system of cd4+t cells, in: 16th International Conference on Control, Automation and Systems (ICCAS), IEEE, 2016.

[31] M. Arsalan, X. Yu, M. T. Sadiq, Development of novel reinforcement learning-based optimizer to impede tumor growth via radiochemotherapy, Scientrific Reportsdoi:https://doi.org/10.1038/s41598-026-56355-2.

[32] A. Hamza, et al, Fuzzy logic and lyapunovbased nonlinear controllers for hcv infection, IET Systems Biology 15 (2021) 53–71. doi:10.1049/syb2.12014.

[33] M. Arsalan, X. Yu, S. Muhammad, J. Choi, Modeling, control, and management of a nonlinear tumorimmune biological system via adaptive smooth sliding mode radiochemotherapy, Mathematics 14 (16). doi:https://doi.org/10.3390/math14162973.

[34] Y. Wen, X. Lou, W. Wu, B. Cui, Backstepping boundary control for a class of gantry crane systems, IEEE Transactions on Cybernetics 53 (2023) 5802–5814. doi:10.1109/TCYB.2022.3188494.

[35] R. Luo, et al., Hiv model parameter estimates from interruption trial data including drug efficacy and reservoir dynamics, PLoS One 7. doi:10.1371/journal.pone.0040198.

[36] M. Arsalan, X. Yu, M. T. Sadiq, A. Almogren, Simultaneous multi-treatment strategy for brain tumor reduction via nonlinear control, Brain Sciences 15. doi:https://doi.org/10.3390/brainsci15020207.

[37] M. Arsalan, S. Muhammad, M. T. Sadiq, Nonlinear smooth sliding mode control framework for a tumor-immune dynamical system under combined radio-chemotherapy, Mathematics 14. doi:https://doi.org/10.3390/math14030521.

[38] A. Javadi, F. Keighobadi, V. Nekoukar, M. Ebrahimi, Finite-Set Model Predictive Control of Melanoma Cancer Treatment Using Signaling Pathway Inhibitor of Cancer Stem Cell, IEEE/ACM Transactions on Computational Biology and Bioinformatics 18 (4) (2021) 1504–1511. doi:10.1109/TCBB.2019.2940658.
URL https://ieeexplore.ieee.org/document/8827909/

[39] M. F. Villa-Tamayo, A. J. N. Anelone, P. S. Rivadeneira, Tumor Reduction Using Oncolytic Viruses Under an Impulsive Nonlinear Estimation and Predictive Control Scheme, IEEE Control Systems Letters 5 (5) (2021) 1705–1710. doi:10.1109/LCSYS.2020.3043185.
URL https://ieeexplore.ieee.org/document/9286591/

[40] US Food and Drug Administration, HIV and AIDS: Medicines to Help You (2020).
URL https://www.fda.gov/consumers/free-publications-women/hiv-and-aids-medicines-help-you

[41] Zhengtong Lv. and Y. Chu and Y. Wang, Hiv protease inhibitors: a review of molecular selectivity and toxicity, HIV AIDS (Auckl) 7 (2015) 95–104. doi:10.2147/HIV.S79956.

[42] Medscape, HIV and AIDS: Medicines to Help You (2023).
URL https://reference.medscape.com/drug/reyataz-atazanavir-342608

[43] US Food and Drug Administration, REYATAZ (atazanavir sulfate) Capsules (2011).
URL https://www.accessdata.fda.gov/drugsatfda_docs/label/2011/021567s026lbl.pdf

[44] US Food and Drug Administration, REYATAZ (atazanavir sulfate) Capsules (2006).
URL https://www.accessdata.fda.gov/drugsatfda_docs/label/2006/021567s007lbl.pdf

[45] J. A. Perez-Molina, et al, Contribution of low cd4 cell counts and high human immunodeficiency virus (hiv) viral load to the efficacy of preferred first-line antiretroviral regimens for treating hiv infection: A systematic review and meta-analysis, Clinical Infectious Diseases 76 (2021) 2027–2037. doi:10.1093/cid/ciad177.

[46] J. S. Altamirano-Flores, S. E. Guerra-Palomares, et al, Identification of hiv-1 vif protein attributes associated with cd4 t cell numbers and viral loads using artificial intelligence algorithms, IEEE Access 8 (2020) 87214–87227. doi:10.1109/ACCESS.2020.2992240.

[47] D. Shi, S. Ma, Q. Zhang, Sliding mode dynamics and optimal control for hiv model, Mathematical Biosciences and Engineering 20 (2023) 7273–7297. doi:10.3934/mbe.2023315.

[48] D. Finzi, et al., Latent infection of cd4+ t cells provides a mechanism for lifelong persistence of hiv-1, even in patients on effective combination therapy, Nature Medicine 5 (1999) 512–517. doi:https://doi.org/10.1038/8394.

[49] R. Colgrove, A. Japour, A combinatorial ledge: reverse transcriptase fidelity, total body viral burden, and the implications of multiple-drug hiv therapy for the evolution of antiviral resistance, Antiviral Research 41 (1) (1999) 45–56. doi:https://doi.org/10.1016/S0166-3542(98)00062-X.
URL https://www.sciencedirect.com/science/article/pii/S016635429800062X

[50] R. Luo, L. Cannon, J. Hernandez, M. J. Piovoso, R. Zurakowski, Controlling the evolution of resistance, Journal of Process Control 21 (3) (2011) 367–378, thomas McAvoy Festschrift. doi:https://doi.org/10.1016/j.jprocont.2010.11.010.
URL https://www.sciencedirect.com/science/article/pii/S0959152410002283